INTERNATIONAL ACADEMIC STUDIES IN ELECTRICAL AND ELECTRONICS ENGINEERING

June 2024

EDITOR

ASSOC. PROF. DR. HİLMİ ZENK

INTERNATIONAL ACADEMIC STUDIES IN ELECTRICAL AND ELECTRONICS ENGINEERING

June 2024

Editor

ASSOC. PROF. DR. HİLMİ ZENK

Contents

Chapter 1

ESTIMATION OF ENERGY PRODUCTION BY ARTIFICIAL NEURAL NETWORKS IN HYDROELECTRIC POWER PLANTS

Erkam Yusuf ISIK[1]

Naim Suleyman TING[2]

Fulya ASLAY[3]

1 M.Sc. Student, Erzincan Binali Yildirim University, Institute of Science and Technology, Department of Electrical Electronics Engineering, isikerkamyusuf@gmail.com, ORCID: 0000-0002-5488-0512
2 Assoc. Prof. Dr., Erzincan Binali Yildirim University, Faculty of Engineering - Architecture, Department of Electrical Electronics Engineering, nsuleyman@erzincan.edu.tr, ORCID: 0000-0003-3743-0824.
3 Assoc. Prof. Dr., Erzincan Binali Yildirim University, Faculty of Engineering - Architecture, Department of Computer Engineering, faslay@erzincan.edu.tr, ORCID: 0000-0001-5212-6017.

1. INTRODUCTION

The rapid increase in the world population, industrialization and technological developments lead to a rapid increase in energy demand worldwide. Increasing energy demand causes excessive use of primary resources such as carbon-based natural gas, oil and coal. With the knowledge that carbon-based fossil fuels are limited and the extent of damage caused by these resources to nature has increased, a global search for sustainable clean energy has begun. Renewable energy sources are important in the search for clean energy. Renewable energy sources such as wind energy, solar energy and hydroelectric energy offer long-term and environmentally friendly solutions. Therefore, it is important to develop, use efficiently and promote renewable energy resources in order to reduce dependence on fossil fuels and support environmental sustainability (Sun and Bae, 2022). Energy, which is considered a strategic concept for the continuity of the life cycle and the development of countries both in the social and economic fields, is provided from carbon-based fuels such as oil, natural gas and coal in nowadays. According to Global Condition, more than 70% of the electricity supply and demand is achieved by using these fuels (Enshaei et al., 2017).

Energy production from renewable energy is very important owing to the demand for energy increasing day by day. Wind, solar and hydroelectric power plants are important in terms of ease of applicability and efficiency of renewable energy sources. The main problems experienced in renewable energy production plants from planning to production transition are the size of the renewable energy capacity, the sudden change in capacity and the model design resulting from those changes. Sudden changes observed in factors such as wind speed, rainfall amount and cloudiness rate directly affect the reliability of the model to be designed. If the production amount of renewable energy production plant cannot be estimated accurately due to meteorological data, the production amount of power plant, the capacity and types of electromechanical equipment to be used may be selected incorrectly. Additionally, it may cause incorrect calculations of investment size and production costs. Electricity production estimating is made based on the analysis of previous year's data and parameters affecting energy production based on data mining principles and evaluation of the results. While only load data sets from past periods are examined in load demand forecast studies conducted in past periods; it is tried to increase the prediction realization rate by including temperature numerical values, percentage relative humidity rates, pressure values, precipitation amounts, increase and decrease rate in national income, changes in exports and unit prices of unprocessed materials used for production in nowadays. While regression analysis method is mostly used in energy load estimation, machine learning techniques used with the widespread use of artificial intelligence techniques produce reliable results in load amount estimation.

Making forward-looking estimates is of great importance in terms of prioritizing investments and providing resource for ensure continuity in energy production in electricity markets. Moreover, reliable and accurate forecasting of electricity production will enable the use of variable electricity sales unit prices to generate high returns. The sales price of the produced electricity is announced in the Transparency Platform of the Energy Markets Operation Company (EMOC) 1 day in advance in the Day Ahead Market in hourly form. EMOC provides unit prices for electricity sales through this system. It requests producers to commit to the energy they can produce on an hourly basis through this system within the scope of these prices. Companies can make healthy and reliable energy production estimates with the correct estimation method. In addition, while the renewable energy power plants are performing their day-ahead market supply, they are required to estimate the electrical energy they will undertake within the scope of the "Regulation on Documentation and Support of Renewable Energy Resources".

Machine learning is an important technology for analyzing data sets very well and organizing the stages of getting results. It is constantly developing and has an important place in academic and industrial studies. One of the methods of machine learning is the artificial neural network method. Artificial neural networks are computer techniques developed in the structure of biological neural networks in order to perform the features such as producing and revealing new information with the learning technique of the human brain without any help. Artificial neural networks, which are a field of study in the science of artificial intelligence, consist of certain techniques for computers to learn. While computers are used only to make calculations and transfer data in the past, today they have become capable electronic machines that summarize large amounts of data sets and draw conclusions about the situation related to these data sets (Ağyar, 2015). ANN tries to perform learning, generalization and remembering processes, which are characteristics of the human brain. ANN forms the basis of the algorithms it uses when performing its learning function with mathematical formulas (Kabalcı, 2014). If there are data sets with nominal values in the data sets to be used, they need to be converted to numerical values because ANN only works with numerical data sets (Ağyar, 2015). ANN performs learning after being trained with some sample patterns and produces results with input data sets after the learning process.
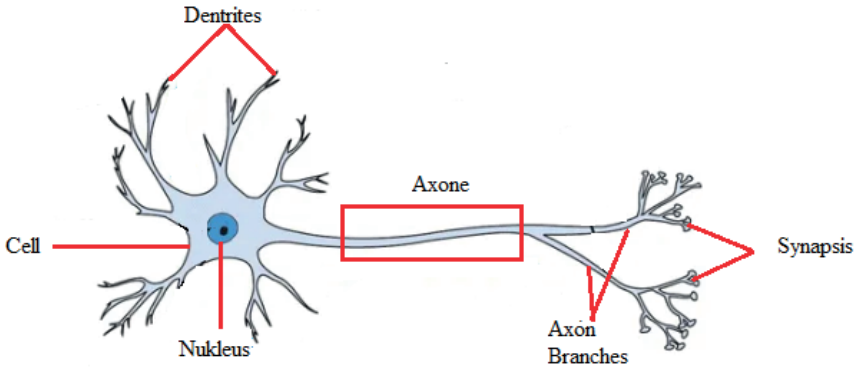
Figure 1. *Biological Nerve Cell*

The biological nerve cells in the human brain shown in Figure 1 are connected to each other by axons. Thanks to these axons, data flow between cells is provided. An artificial neural network, similar to the human brain, consists of many nerve cells connected in parallel to each other to form neurons. The learning data sets obtained during ANN training are stored on the new network formed between neurons (Erbaş, 2015). The shape shown in Figure 2 is a nerve cell belonging to a simple ANN structure. The inputs created with external data sets shown by X are the weights of different values shown by W. It consists of five main components: the aggregation function where all the weights are brought together, the activation (transfer) function used to create the result, and the output function (Esen, 2023).

The information given to the cells from outside constitutes the inputs in ANN application. These inputs or data sets from the previous layer are transmitted to the cells of the artificial neural network as input data (Özveren, 2006:7). These inputs are shown with the symbol Xi and are multiplied by the weight (wij) specified in equation (1) and added to the threshold value (bj). Weights show the importance of the incoming data of an artificial neural network and the effect it creates on the neuron (Öztemel, 2013: 90). Weights (w1, w2, w3…… wi ,) are appropriate coefficients that determine the effect of the inputs received by the artificial neural network on the neuron (Elmas, 2013: 35).

$$Zi = \sum_{i=1}^{n} (wijxi + bj) \qquad 1)$$
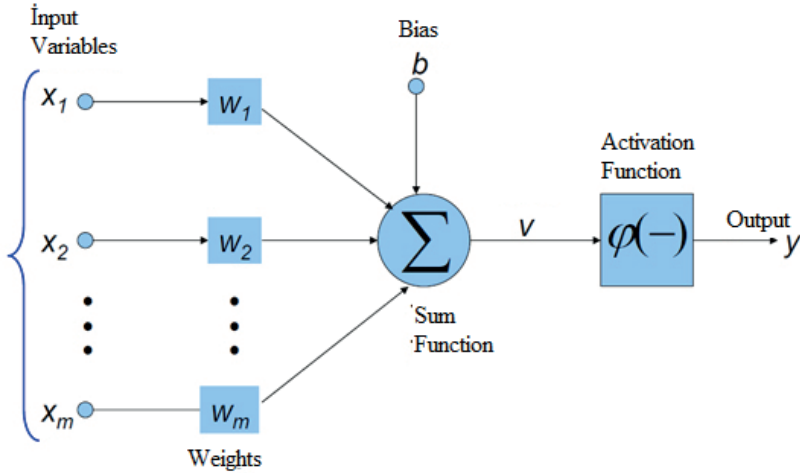
Figure 2. *Artificial Neural Network Model Structure (Esen, 2023).*

Learning in ANN models is done in two ways. These learning methods are called supervised and unsupervised. While the input and output values are given to the model together in the supervised learning technique, the learning process is carried out by establishing the connection between the input and output data sets given to the system. The weights between data sets are randomly adapted by the network. Only input data sets are given to the model and the model is expected to produce an output data in unsupervised learning (Öztemel, 2003). They used water amount, monthly reservoir water level height, and specific water factor data as input in the neural network model they created to estimate the energy production values of the HPP and increase efficiency. They concluded that a safe energy production estimate ismade by increasing the production efficiency of the HPP by looking at the output data (Wang et al., 2020). Energy production companies use load forecasting methods in order to predict the load supply and demand amount and manage their resources well. Distribution companies use load forecasting methods to reduce congestion and overload by optimizing the energy flow of transmission lines.

In this study, an energy consumption forecast is made for Short-Term Production Forecast (STPF) and Medium-Term Production Forecast (MTPF) in HPPs using machine learning algorithms. Meteorological data of the Ergan Ski Center station, located at station number 17983, belonging to the Erzurum 12th Regional Directorate of the Republic of Turkey, Ministry of Environment, Urbanization and Climate Change, are used in the study. These data are used as meteorological forecast data. Besides, 8 different data covering the years 2006-2022 belonging to the Yukarı Mercan HPP located

in the Central Günbağı Village of Erzincan province, namely the Amount of Water Converted to Energy (m³), Average Pool Height (m), Average Net Head (m), Average Flow Rate (m3), OSF Values (Invoice Basis), Power Plant Internal Needs Meter Active Consumption (kWh), Specific Water Factor (m3/Mw) and Gross Production data are used.

2. SHORT-TERM AND MEDIUM-TERM ENERGY PRODUCTION FORECASTING USING ARTIFICIAL NEURAL NETWORKS METHOD

The *sim* function, which allows creating models with the Artificial Neural Network Method with MATLAB R2020a ®, isused. The *sim* function is applied to simulate the neural network on the input data and produces the output values of the data belonging to the predicted values. The *HiddenLayerSize* variable defines the number of neurons in the hidden layer of the neural network model, and in the context of neural networks, this hidden layer is the layer between the input and output layers where the model learns to capture complex patterns in the data. The number of neurons in the hidden layer isset to 21 in study. The selection of the number of neurons in the hidden layer is a hyperparameter that you can adjust according to the characteristics of the data and the complexity of the data. The cell array transfer function (TF) is defined as the transfer function for the layers in our neural network in MATLAB. The functions 'tansig' and 'purelin' are defined in the TF. 'tansig' is the hyperbolic tangent sigmoid transfer function. It is often used in hidden layers as it maps input values to a range between -1 and 1, which can help train neural networks. The 'purelin' function is a linear transfer function typically used in the output layer for regression tasks. In other words, it calculates a linear combination of the inputs.

As training parameters;

- net7t.trainParam.lr = 0.01; %Learning rate
- net7t.trainParam.epochs = 1000; % Number of training epochs
- net7t.trainFcn = 'trainlm'; % Levenberg-Marquardt

are used.

The train function is used to train the neural network using the specified training data. The details of the training process, such as the selection of the optimization algorithm, the learning rate, and the number of epochs, depend on the default settings or the values to be predicted for the neural network before training, the training parameters, and the actual values to be predicted. While the Artificial Neural Network Method, which is studied, isbeing studied for short-term, which consist of 30 days, and medium-term, consist of 90 days and 180 days, load estimations; MAPE, MAE, MSE, and RMSE results and graphs are created with estimated and real values. Using

the table values and graphs in medium-term load estimation would give us more stable and reliable values. The values to be used are first used in the testing phase and then the estimate is made using 16 years of data values.

2.1. 30 Days Production Prediction Application for STPF

30 days short term load forecast is made using ANN method in MATLAB program with script. The success rate of the study isdetermined with MAPE, MAE, MSE and RMSE performance functions. MAPE, MAE, MSE and RMSE performance values are shown in Table 1. The training iscarried out according to the Levenberg-Marquardt model and iscarried out without using meteorological data (with 11 parameters) and using the data of HES (with 6 parameters).

Table 1. *Evaluation of 30 Days SPFF Model Performances*

Performance Function	Value
MAPE	0.106711885573285
MAE	6.6247671514e-05
MSE	1.454370153e-07
RMSE	0.033041503396976

17 variables are used input values ANN model for 30 days electricity production prediction. The hiddenlayer isset to 21 for obtaining reliable value. The results of the 30 days electricity production forecast study using artificial neural networks are shown in Table 1 and Figure 3 - Figure 5. The aim of the ANN model is obtained output value which is production electricity value in Figure 3. The Levenberg-Marquardt (LM) algorithm used in modeling is preferred due to the speed and stability it provides in the training of artificial neural networks. The artificial neural networks 30-day prediction data graph in Figure 5., RTtestY30 value is the actual data value and yPredANN30 is the predicted value.
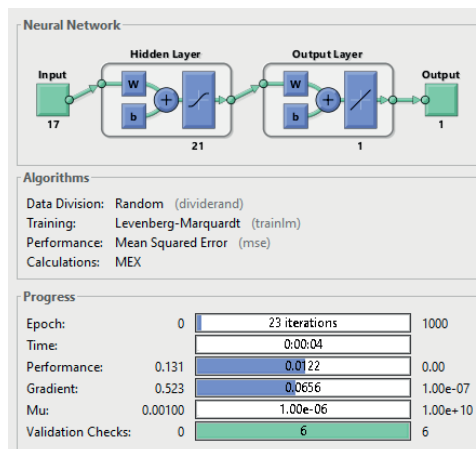
Figure 3. *ANN Training for 30 Days Prediction*
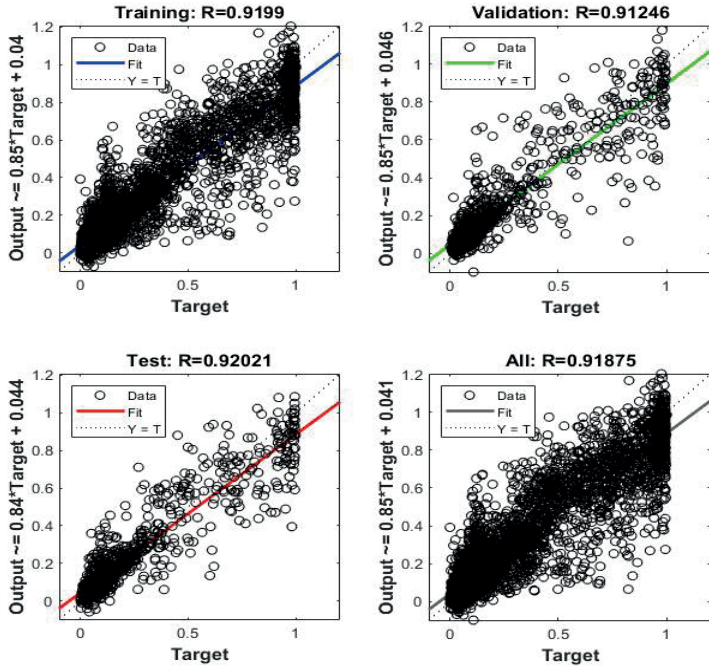
Figure 4. *Regression Graphics for 30 Day Prediction*
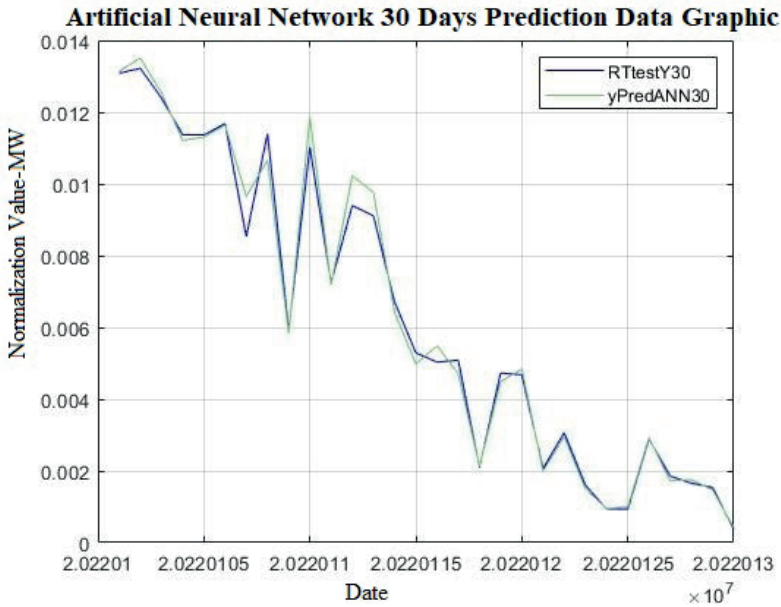
Figure 5. *30 Days Prediction Graphic*

2.2. 90 Days Production Prediction Application for MTPF

90 days midium term load production ismade using ANN method in MATLAB program with script. The success rate of the study isdetermined with MAPE, MAE, MSE and RMSE performance functions. MAPE, MAE, MSE and RMSE performance values are shown in Table 2. The training iscarried out according to the Levenberg-Marquardt model and iscarried out without using meteorological data (with 11 parameters) and using the data of HES (with 6 parameters).

Table 2. *Evaluation of 90 Days MTPF Model Performances*

Performance Function	Value
MAPE	2.5493984956318
MAE	0.140764263553384
MSE	0.049966021877782
RMSE	0.2067909251702

17 variables are used as input values ANN model for 90 days electricity production prediction. The hiddenlayer isset to 21 for obtaining reliable value. The results of the 90 days electricity production forecast study using ANN are shown in Table 2 and Figure 6 - Figure 8. The aim of the ANN model is obtained output value which is production electricity value in Figure 6. The artificial neural networks 90 days prediction data graph in Figure 8., RTtestY90 value is the actual data value and yPredANN90 is the predicted value.
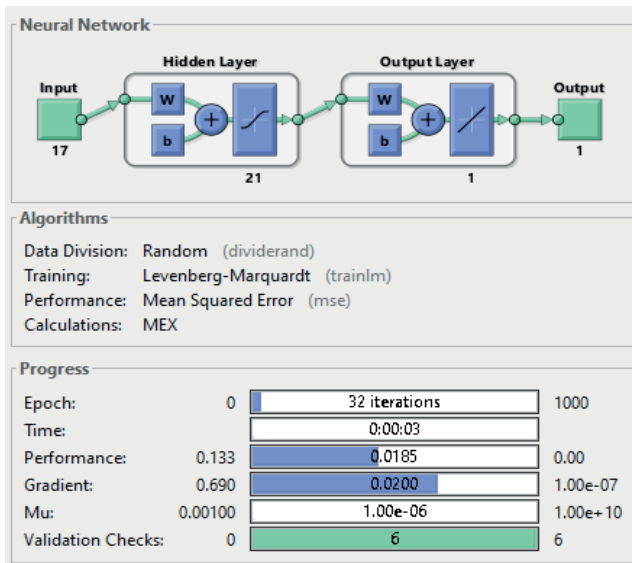
Figure 6. *ANN Training for 90 Days Prediction*
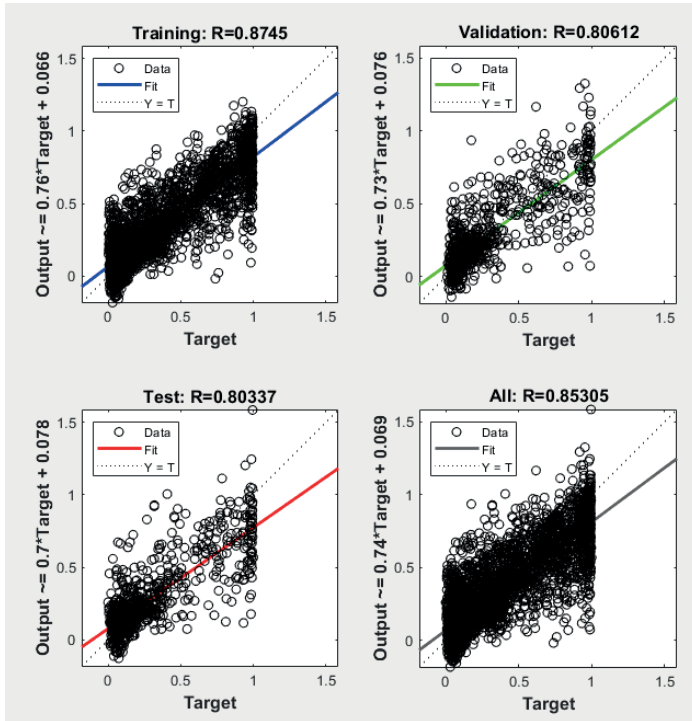
Figure 7. *Regression Graphics for 90 Day Prediction*
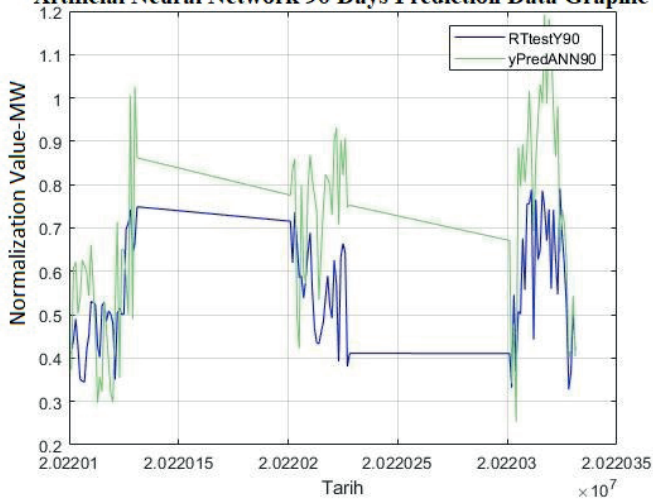
Figure 8. *90 Days Prediction Graphic*

2.3. 180 Days Production Forecast Application for MEPF

180 days midium term load production ismade using ANN method in MATLAB program with script. The success rate of the study isdetermined

with MAPE, MAE, MSE and RMSE performance functions. MAPE, MAE, MSE and RMSE performance values are shown in Table 3. The training iscarried out according to the Levenberg-Marquardt model and iscarried out without using meteorological data (with 11 parameters) and using the data of HES (with 6 parameters). 17 variables are used as input values ANN model for 180 days electricity production prediction. The hiddenlayer isset to 21 for obtaining reliable value. The results of the 180 days electricity production forecast study using ANN are shown in Table 3 and Figure 9 - Figure 11. The aim of the ANN model is obtained output value which is production electricity value in Figure 9. The ANN 180 days prediction data graph in Figure 11, RTtestY180 value is the actual data value and yPredANN180 is the predicted value.

Table 3. *Evaluation of 180 Days MTPF Model Performances*

Performance Function	Value
MAPE	5.557952252048338
MAE	0.173301359561225
MSE	0.06826020175856
RMSE	0.2816870532030
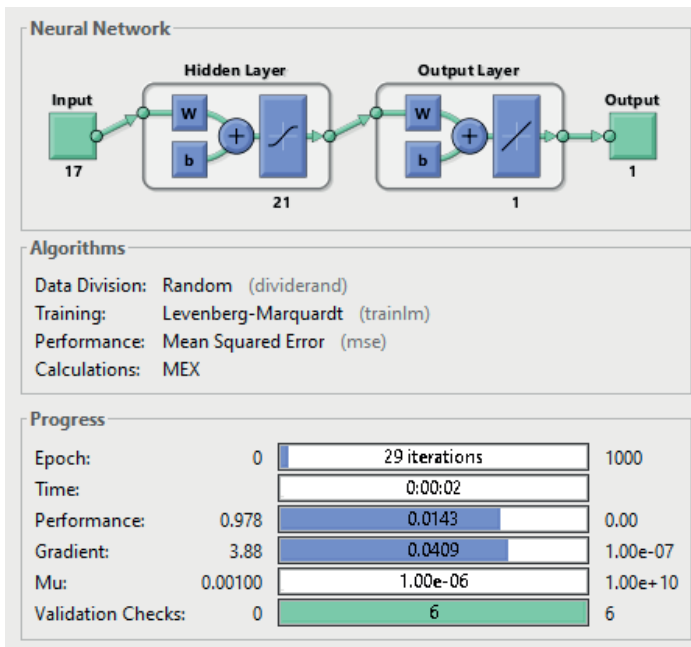
Figure 9. *ANN Training for 180 Days Prediction*
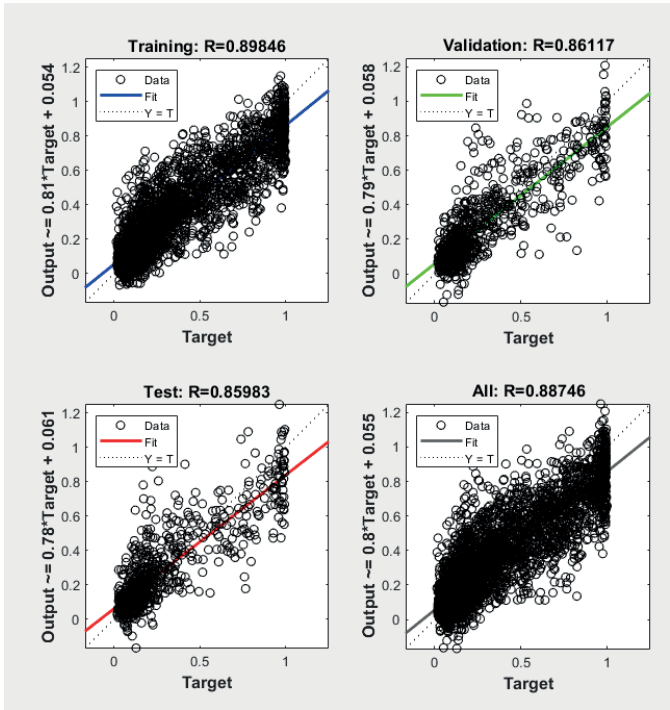
Figure 10. *Regression Graphics for 180 Days Prediction*
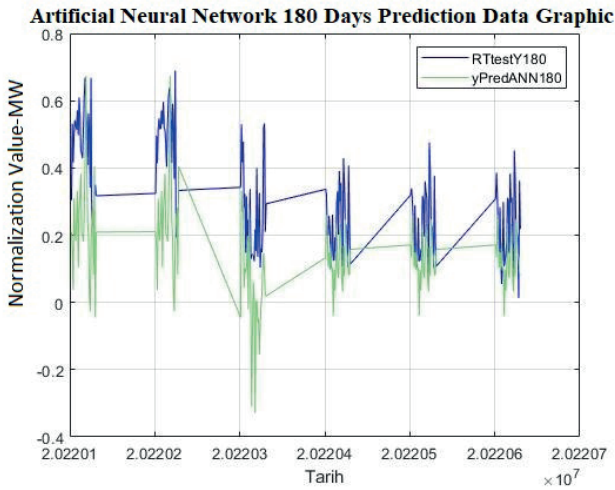
Figure 11. *180 Days Prediction Graphic*

3. CONCLUSION

In this study, SPFF and MEPF studies are conducted for HPP with ANN which is a method of machine learning methods. Modeling with ANN is designed using a channel type HPP and meteorological station data close to the HPP location. The aim of the study conducted using the method and data is to determine the most appropriate method for SPFF and MEPF and to use it in energy production estimates. In the HPP where the study isconducted, production and budget programs are used in 1-month, 3-month (90-day quarters) and 6-month (180-day) periods (to be used in studies such as the 1st half and 2nd half of the year).

A MAPE value below 10% indicates high predictive success (Tekin and Patır, 2023). A MAPE value below 10% is considered "very good", between 10% and 20% is considered "good", between 20% and 50% is considered "reasonable", and above 50% is considered "bad" (Aslay, 2013).

When the performance tables are examined, it has been determined that the prediction study made with artificial neural networks is the ideal method for short-term and medium-term forecasting studies, considering the MAPE value, which is one of the performance functions. However, among the 3 estimation methods, the closest estimation value to the actual value isobtained in the 30 days short-term load estimation study. Root Mean Square Error (RMSE) is calculated as a measure of accuracy. The smaller the RMSE value, the closer the predicted value is to the true value. The coefficient of the regression study is considered as an indicator of the prediction accuracy of the multi-year measurement (R^2). The smaller the R^2 value, the closer the predicted value is to the true value (Li, 2020).

When the RMSE performance result values are examined, it isdetermined that the 30-day forecast study isthe modeling that reached the closest to the actual values. When examined according to R performance result graphs, it isdetermined that the 30 days forecast study isthe modeling that reached the closest to the actual values. It has been observed that the ANN algorithms modeled in the estimation studies generally work correctly. The fact that the ANN algorithm can take a rote approach in large and repetitive data is among the disadvantages of the algorithm. In terms of modeling speed, ANN algorithms can provide fast and practical solutions.

REFERENCES

Sun, Z. and Bae, S. (2022) "Multiple-Input Soft-Switching DC–DC Converter to Connect Renewable Energy Source in a DC Microgrid", *IEEE Access*, 10, 128380-128391.

Enshaei, K., Monaaf, D.A. and Jayasinghe, S.D.G. (2017) "A Review on Recent Size Optimization Methodologies for Standalone Solar and Wind Hybrid Renewable Energy System", *Energy Conversion and Manegement*, 143, 252-274.

Ağyar, Z. (2015) "Areas of Use of Artificial Neural Networks and an Application", *Engineer and Machinery*, 56(662), 22-23.

Kabalcı, E. (2014). "Artificial Neural Networks",

https://ekblc.files.wordpress.com/2013/09/ysa.pdf,

Date of Access: 11.04.2024.

Erbaş, Ü. (2015). "Artificial Neural Networks and Application Areas", PhD Thesis, *Marmara University Institute of Social Sciences*, Istanbul.

Esen, A. (2023). "Main Elements of Artificial Neural Network",

https://www.akanesen.com/2017/09/yapay-sinir-agnn-ana-ogeleri.html,

Date of Access: 15.03.2024.

Öztemel, E. (2003). "Artificial Neural Networks", Papatya Publishing, Istanbul.

Wang, Y., Liu, J. and Han, Y. (2020). "Production Capacity Prediction of Hydropower İndustries For Energy Optimization: Evidence Based on Novel Extreme Learning Machine İntegrating Monte Carlo" *Journal of Cleaner Production*, 272 (2020), 122824.

Özçelik, E. and Özveren, E. (2006) "An Institutionalist Perspective on the Future of the Capitalist World-economy", *Journal of Economic Issues*, 40 (2), 413-420.

Elmas, L., Akcılar, R., Turgut, S., Caner, V., Akcılar, A., Ayada, C., and Özcan, T. O. (2013). "Apelin Effects on Blood Pressure and RAS in DOCA-Salt-Induced Hypertensive Rats" *Clinical and Experimental Hypertension,* 35(7), 550–557.

Aslay, F. (2013). "Estimation of Soil Temperature with Artificial Neural Networks Using Meteorological Parameters", *PhD Thesis, Ataturk University Institute of Social Sciences*, Erzurum.

Li C., (2020). "Biodiversity Assessment Based on Artificial İntelligence and Neural Network Algorithm" *Microprocessors and Microsystems* 79, 103321

Chapter 2

DRIVING RANGE EXTENSION OF ELECTRIC VEHICLES WITH WIND GENERATOR SUPPORT

M.Murat TEZCAN[1]

Taha Melih KARAMAN[2]

1 (Ph.D.), Kütahya Dumlupınar University Faculty of Engineering, Dept. of Electrical Electronics Engineering, ORCID ID: 0000-0002-5390-4527, murat.tezcan@dpu.edu.tr

2 (Bs.C.), Kütahya Dumlupınar University Faculty of Engineering, Dept. of Electrical Electronics Engineering, ORCID ID: 0009-0009-8929-2874, karamantahamelih@gmail.com

1) Introduction

The global surge in the adoption of electric vehicles (EVs) signifies a transformative shift towards sustainable transportation solutions. At the heart of this paradigm shift lies the imperative to mitigate the adverse environmental impacts associated with traditional internal combustion engine vehicles. Internal combustion engines increase carbon emissions and cause air pollution due to fossil fuel consumption. This accelerates global warming, contributing to climate change and negatively impacting human health [2]. Thus, the search for environmentally friendly transportation solutions has further heightened the importance of electric vehicles.

The rise of electric vehicles is underpinned by their intrinsic eco-friendly attributes, which render them indispensable agents in the global quest for environmental conservation and climate resilience. EVs operate with zero exhaust emissions, improving air quality and reducing the carbon footprint. Furthermore, when charged with renewable energy sources, they further diminish dependence on fossil fuels, creating a sustainable energy cycle.

However, despite their burgeoning popularity, EVs grapple with certain inherent limitations, chief among them being the constraint on operational range. The distance that electric vehicles can travel on a single charge is still limited compared to internal combustion engine vehicles. This situation, especially for long-distance travel, causes users to worry and emerges as one of the biggest obstacles to the widespread adoption of EVs. Recognizing this challenge as a critical barrier to widespread adoption, stakeholders across industries are actively engaged in multifaceted research endeavors aimed at surmounting the range limitation.[3]

Figure -1 *Electric Vehicle [4]*

Renewable energy sources emerge as linchpins in this quest for extending the operational capabilities of EVs. Solar power, with its inexhaustible potential, and wind energy, harnessing the kinetic force of the atmosphere, stand out as promising avenues for augmenting the energy reservoirs of electric vehicles. The integration of solar panels into the bodywork of EVs and the deployment of low-power wind turbines strategically positioned to capture airflow during motion present innovative solutions to bolstering energy reserves. Solar panels can continuously generate energy even while the vehicle is in motion, thereby increasing battery capacity and extending range. Wind turbines, on the other hand, provide additional energy by harnessing the airflow generated while the vehicle is moving. These innovative solutions have the potential to significantly mitigate the range limitation of EVs.[5]

Furthermore, advancements in battery technology play a pivotal role in enhancing the viability of electric vehicles for long-distance travel. Breakthroughs in lithium-ion battery design, coupled with advancements in solid-state battery technology, promise higher energy densities and faster charging capabilities, thereby alleviating range anxiety among consumers. Lithium-ion batteries, the most commonly used type, are notable for their energy density and long lifespan. Solid-state batteries offer even higher energy densities, reduce fire risk, and can charge faster. These technological advancements enable electric vehicles to cover longer distances in shorter times, enhancing the user experience.[6]

Figure -2 *Electric Vehicle [7]*

Moreover, policy frameworks aimed at incentivizing EV adoption and fostering research and development initiatives play a pivotal role in shaping the trajectory of sustainable transportation. Subsidies, tax incentives, and regulatory mandates aimed at reducing emissions and promoting clean energy adoption serve as catalysts for market penetration and technological innovation in the EV sector. Governments and international organizations offer various incentives to accelerate the adoption of electric vehicles, guiding

both manufacturers and consumers toward EVs. These incentives include tax reductions on vehicle purchases, financial support for charging station installations, and regulations encouraging the use of electric vehicles. [8]

In tandem with technological advancements and policy support, consumer awareness and acceptance are integral facets of the transition towards electric mobility. Education campaigns highlighting the environmental benefits, cost savings, and technological advancements associated with EVs play a crucial role in dispelling misconceptions and fostering a culture of sustainability-conscious consumerism. These campaigns promote the advantages of electric vehicles to broader audiences, increasing interest in environmentally friendly and economical transportation solutions. Educating consumers about the long-term cost benefits, low maintenance requirements, and positive environmental impacts of electric vehicles accelerates EV adoption.

2) In conclusion, the journey towards widespread adoption of electric vehicles is characterized by a confluence of technological innovation, policy intervention, and societal acceptance. As stakeholders collaborate to surmount the challenges impeding the mainstream adoption of EVs, the vision of a sustainable transportation ecosystem, powered by renewable energy sources and propelled by electric mobility, inches closer to fruition. This transformation not only provides environmental benefits but also creates positive impacts in economic and social spheres, marking a significant step towards a cleaner, more efficient, and more sustainable future.[9]

2) Electric Vehicles

Electric vehicles are a type of vehicle that operates using electricity instead of gasoline or diesel. They work by employing an electric motor for power generation and utilize rechargeable batteries to store the energy produced by the motor. Electric vehicles are generally quieter and more reliable than traditional gasoline- powered vehicles, and they require less maintenance.

The biggest drawback of electric vehicles is their inability to store enough energy to keep the vehicle running for long periods. The energy storage capacity of batteries used in electric vehicles is significantly lower compared to the conventional fuels used in modern automobiles. While the operation, performance, and efficiency of electric motor vehicles are much better than those powered by internal combustion engines, electric vehicles are environmentally friendly. However, electric vehicles still lag behind in the automotive sector due to the energy storage issue. Internal combustion engine vehicles emit harmful gases, making electric vehicles crucial for protecting both the environment and human health today. Nevertheless, the biggest challenge for electric vehicles is their range limitation. [10]

Figure -1 *Electric Vehicle Chassis [11]*

Many electric vehicle manufacturers offer a warranty for the first 4 years of usage, guaranteeing the battery's capacity to remain at 80%. Electric vehicles provide users with the opportunity to save on fuel costs. The equivalent of 1 liter of gasoline consumed by an internal combustion engine vehicle is determined to be 10 kWh in an electric vehicle. An electric vehicle consumes approximately 18 kWh of electric energy for a 100-kilometer driving distance, which signifies significantly lower energy consumption compared to an internal combustion engine vehicle. It has been determined that an internal combustion engine vehicle consumes six times more fuel than this. Many companies around the world are working to eliminate this problem by developing solutions for charging the batteries of an electric vehicle while it is in motion.

Renault	Toyota	Hyundai	VolksWagen	Tesla	General Motors
Renault employs thick cells in its newly developed battery system. These cells enable an increase in energy density and allow for optimization of heat management, charging profile, and memory effect. As a result of this optimization, users' battery lifespan and vehicle range are extended.[12]	Toyota is developing advancements in integrated systems that enable the collaboration of battery pairs. This integrated system not only reduces charging times but also increases energy density. In the battery architecture of the bZ4X, different modular structures are utilized, with cells separated into blocks and supported by cooling channels.[13]	The battery management system can monitor the voltage, current, and temperature levels of each cell in real-time. An optimized charging and discharging profile is created for each cell. The system is also capable of managing the battery's heating/cooling control with artificial intelligence-supported algorithms. This provides users with optimum range and charging time.[14]	The battery system consists of next-generation cells with lithium-ion nano technology, which increases energy density. A compact structure is utilized in the battery module design to provide volume advantage. Additionally, heat management is optimized with a channelled cooling system, and adaptive algorithms are employed to collect charging and usage data for self-charging design implementation.[15]	The high surface area of graphene increases the uptake and release rate of lithium ions when used in Tesla battery technology. This allows for faster charging and higher energy density to be achieved. Even with just a 0.1% addition of graphene, performance can be increased by 10%.[16]	GE is making batteries more efficient by using silicon carbide in battery production to produce longer or similar ranges from a smaller pack. This results in less power loss in cold weather and reduces the risk of catching fire.[17]

Table-1 *Some Range Extension Efforts by Companies*

2.1) Types of Electric Vehicles

Electric vehicles are a type of vehicle that operates solely on electricity or hybrid electric power, unlike gasoline or diesel vehicles. Due to their efficiency, eco-friendliness, and cost savings, electric vehicles have become increasingly popular in recent years. Electric vehicles operate using an electric motor instead of internal combustion engines to generate power. Batteries are used to store the energy produced by the electric motor. Compared to internal combustion engines, electric vehicles are quieter and more reliable. Maintenance costs are also lower compared to other types of engines, requiring less frequent maintenance. Additionally, due to their adherence to zero-emission regulations, electric vehicles are considered a more sustainable option compared to fossil fuel-powered vehicles. [18] Electric vehicles are divided into four as Full Electric Vehicle (BEV), Hybrid Electric Vehicle (HEV), Plug-in Hybrid Electric Vehicle (PHEV) and Fuel Cell Electric Vehicle (FCEV).[19]

2.1.1) Fully Electric Vehicle (BEV)

Completely Electric Vehicles (AEV), also known as Battery Electric Vehicles (BEV), operate entirely with battery and electric powertrain components. These types of electric cars do not have an internalcombustion engine. Electricity is stored in a large battery pack that is charged by being plugged into the electrical grid. The battery pack then provides power to one or more electric motors to operate the electric vehicle. [20] Architecture and Main Components:
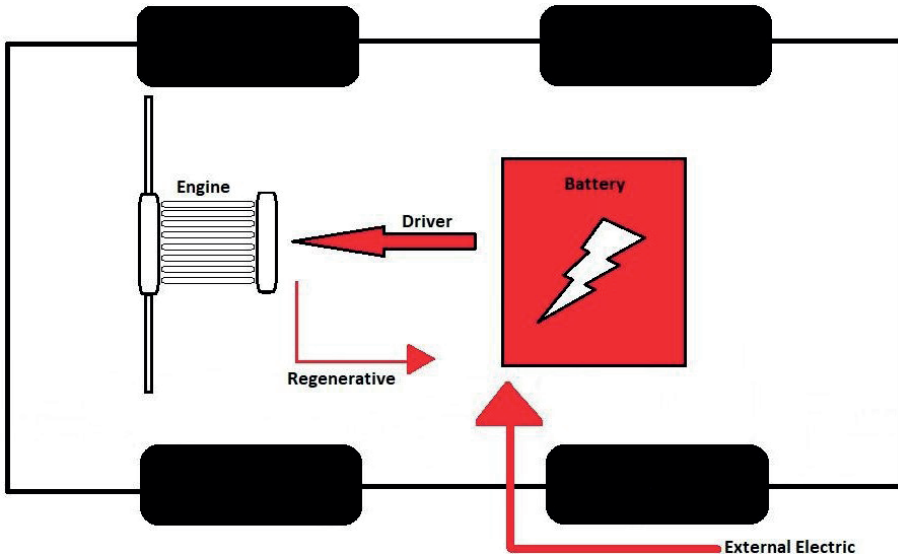
Figure -2 Battery *Electric Vehicle (BEV)*

2.1.2) Hybrid Electric Vehicle (HEV)

These types of hybrid cars are generally referred to as standard hybrids or parallel hybrids. In an HEV, both an internal combustion engine and an electric motor are present. In these types of electric vehicles, the internal combustion engine obtains energy from fuel (such as gasoline and other fuel types), while the electric motor draws energy from the batteries. Both the gasoline engine and the electric motor simultaneously rotate the transmission, which moves the wheels. In hybrid electric vehicles, the regenerative braking system is used to charge the battery. Hybrid electric vehicles are divided into three types series hybrid electric vehicle, parallel hybrid electric vehicle, and series-parallel hybrid electric vehicle. Parallel hybrid electric vehicles are the most common type of hybrid vehicles. In parallel hybrid electric vehicles, the internal combustion engine and the electric motor are connected parallel to the vehicle and provide power together.[20] The difference between HEVs and BEVs/PHEVs is that the batteries in HEVs can only be charged by the internal combustion engine, the movement of the wheels, or a combination of both. Since there is no charging port, it is not possible to charge the battery from outside the system, such as from the electric grid [21].
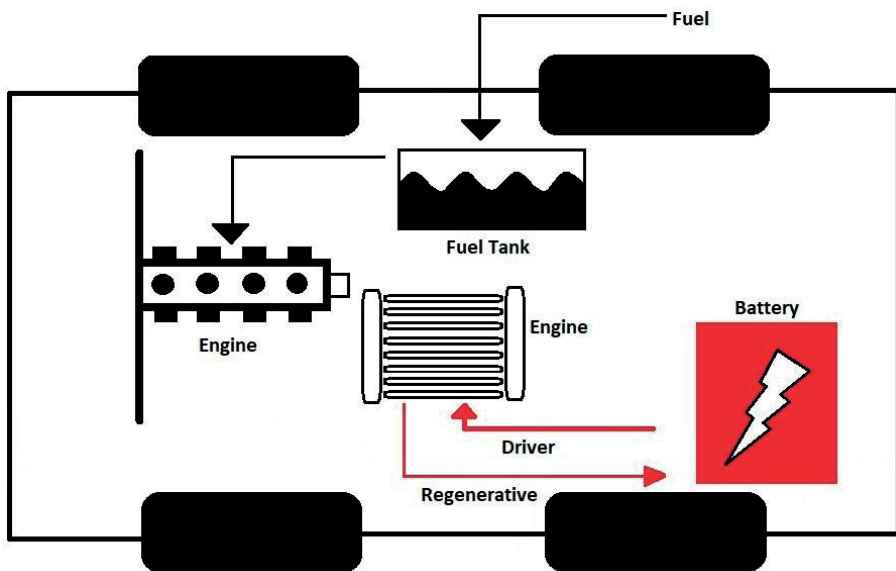
Figure 3. *Hybrid Electric Vehicle (HEV)*

2.1.3) Plug-in Hybrid Electric Vehicle (PHEV)

PHEV, a type of hybrid vehicle consisting of both an internal combustion engine and an electric motor, typically referred to as a series hybrid. Some models switch to hybrid mode when cruising at highway speeds (usually

above 60 or 70 km/h). When the battery is depleted, the engine kicks in and the vehicle operates as a traditional, non-plug-in hybrid. PHEV batteries can be charged not only by connecting to an external power source but also by an internal combustion engine or regenerative braking. During braking, the electric motor acts as a generator to charge the battery using the energy, completing the power of the engine [21].
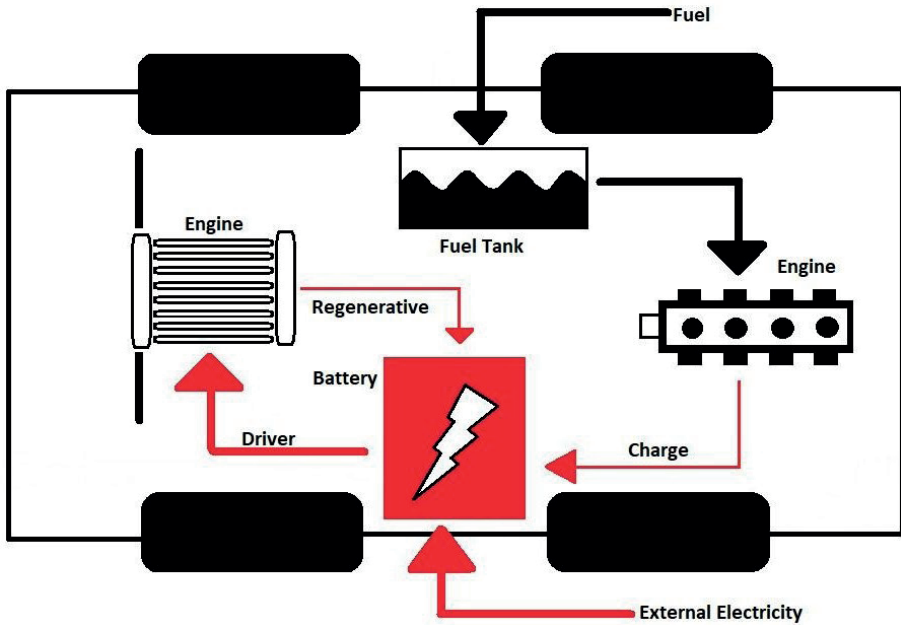
Figure 4. *Grid-Chargeable Hybrid Electric Vehicle (PHEV)*

2.1.4) Fuel Cell (Hydrogen-Powered) Electric Vehicle (FCEV)

Fuel cell vehicles (FCVs) or Fuel Cell Electric Vehicles (FCEVs), also known as Zero Emission Vehicles, are types of electric cars that utilize "fuel cell technology" to generate the electricity needed to power the vehicle. In these types of vehicles, the chemical energy of the fuel is directly converted into electrical energy. The reason for this type of electric vehicle is that FCEVs produce the electricity needed to operate the vehicle within the vehicle itself [21].
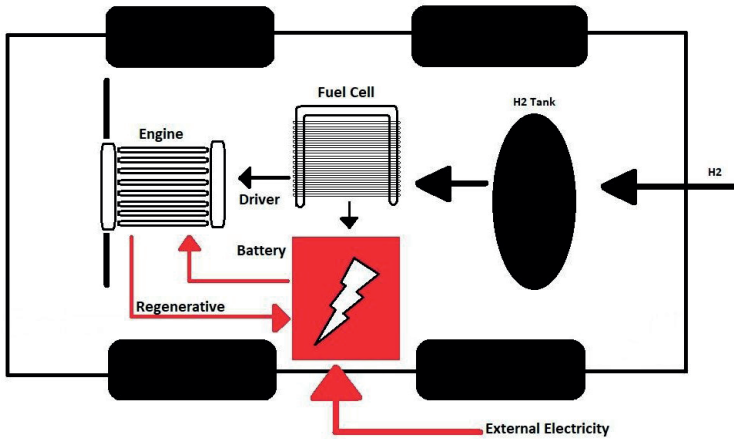
Figure 5. *Fuel Cell Electric Vehicle (FCEV)*

3) Studies About Driving Range Extension in Electric Vehicles

One of the greatest advantages of electric vehicles is their clean energy source and significantly low carbon emissions. Renewable energy sources are the most important means of obtaining energy due to their use of clean energy. Wind turbines, a renewable energy source, have begun to be used and integrated into efforts to extend the range of electric vehicles.

3.1) Suspension Generator (Dynapower)

Firstly, work is being conducted on an experimental Peugeot 308 vehicle equipped with a series of sensors to measure wind speed and road profiles. The wind turbine is designed using CAD software. A classical Luenberger observer is utilized for predicting road slope. Subsequently, the terrain-wheel contact generates generalized forces that can spread to the suspension as kinetic energy. A gear rod system that converts linear motion into rotational motion is utilized for power generation. Both the wind turbines and suspension force form a globally connected system called "DynaPower". The gear mechanism can be fixed to the moving part of the suspension. The gear must be connected to a generator to charge the batteries. Therefore, the batteries will have a continuous power source as long as the vehicle is in motion. The concept of "DynaPower" is established between the suspension device and the wind turbines, aiming to generate power using energy lost from dynamics [22].
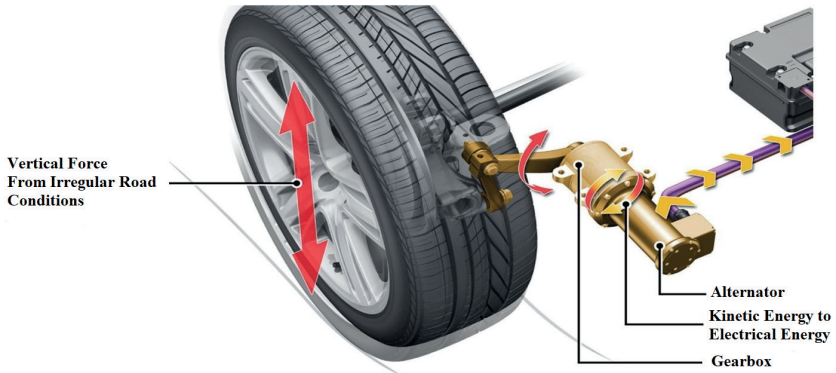
Figure 6. *Suspension Generator Mechanism [23]*

3.2) Integration Study of a Low-Power Wind Turbine onto a Vehicle

It is possible to place wind turbines on the roof of the vehicle without compromising its aerodynamics. This device can be used to capture wind energy and generate power. When the vehicle is in motion, the wind enters from the front into the air channel, causing the turbine blades connected to a generator via a shaft to rotate. The system will be used in specific circumstances. The system consists of two vertical turbines located at the front and rear of the vehicle's roof, small generators, and two honeycomb structures. These structures are used to ensure smooth airflow, maintain vehicle dynamics without disruption, and protect the entire system. The device is intended to be used when the driver brakes, when the vehicle is parked in a safe place, and on inclined roads [24].

Figure 7. *The First Experimental Device [25]*

3.3) Integration Study of Low-Power PMSG Wind Turbine into the Front Ventilation Area of Electric Vehicles

A small Permanent Magnet Synchronous Generator (PMSG) based wind turbine is placed on the front ventilation area and rear of the vehicle, so that some of the kinetic energy of the wind passing through the ventilation channels is recovered.Therefore, the wind turbine not only captures some of the vehicle's kinetic energy losses but also has no effect on the vehicle's aerodynamic coefficient because it is embedded behind the ventilation channels, thus not generating any additional resistance force[26].

3.3.1) Operation Principle of the Front Ventilation Area Battery Charging System

The layout of the battery charging system experimental setup in Figure 8 primarily focuses on the necessity of a system that can charge high-capacity batteries used in Electric Vehicles (EVs) with minimal loss. For this system to provide more benefits to users of these Electric Vehicles, it must be powerful and highly efficient. Comprised of the most efficient components that can provide the required power without affecting the vehicle's performance, this proposed system is suitable for any type of battery used in the automotive sector.
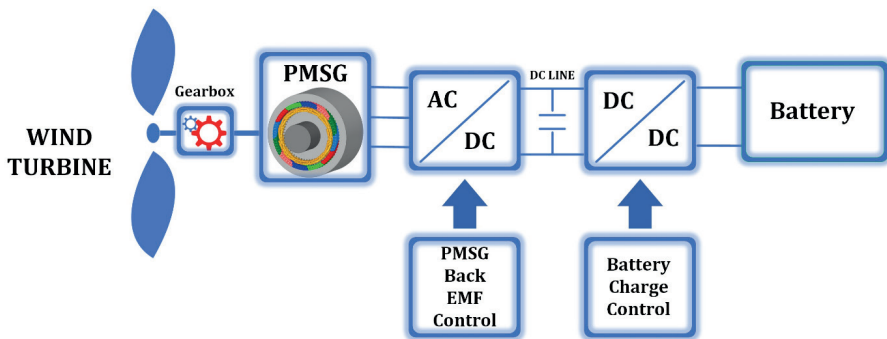
Figure 8. *Experimental Setup Layout [27]*

This system primarily operates based on the speed of the vehicle, so that when the vehicle moves at a certain speed, power generation occurs at that speed, and the power output changes when the speed changes. To address this situation, the system consists of several components that provide continuous and steady power supply to the battery to ensure uninterrupted charging (Figure 9).
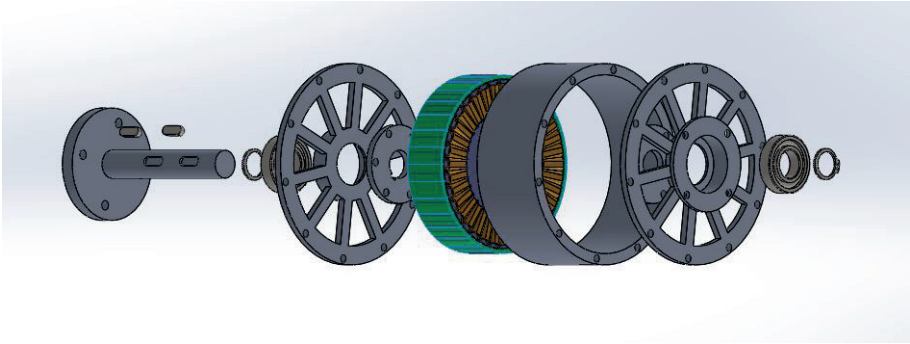
Figure 9. *PMSG Internal Structure*

The proposed battery charging system design is capable of efficiently generating the power output required to charge the batteries used in Electric Vehicles (Fig.10). Although the system is primarily dependent on the constantly changing vehicle speed, it continuously generates a steady power output to ensure uninterrupted battery charging. Low-cost, efficient, clean wind energy-based power generation, along with the placement of the turbine in a high-flow area, is effectively utilized in charging the battery [28].
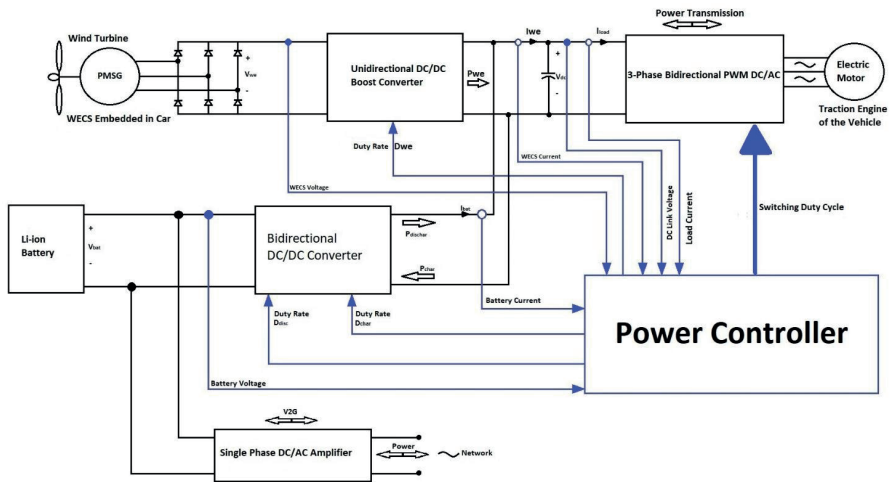
Figure 10. *Wind Turbine Supported Battery Charging System Network*

The electrical circuit of the battery converter is illustrated in Figure 11. It is a bidirectional boost-buck converter. As shown in Figure 11, in the charging direction, it operates as a buck converter with Dchar charge duty cycle, while in the discharging direction, it operates as a boost converter with Ddisc discharge duty cycle.
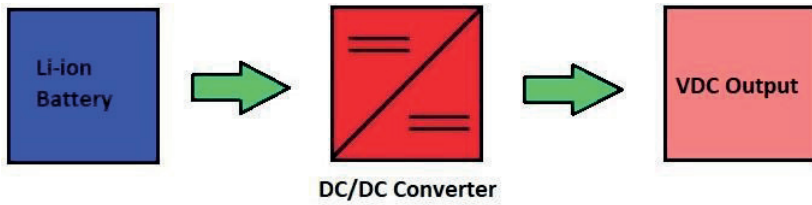
Figure 11. *Battery Charger Converter Block Diagram*

The detailed structure implementing the proposed system has been built with a prototype system placed inside the EV. The constructed WECS is a wind turbine. As seen in Figure 12, by placing the wind turbine in the front ventilation channel of the vehicle, the vehicle can charge the battery both while in motion and when stationary, using the wind coming from outside. This means that the wind turbine does not generate any additional resistance force, hence it has no effect on the aerodynamic coefficient of the vehicle.
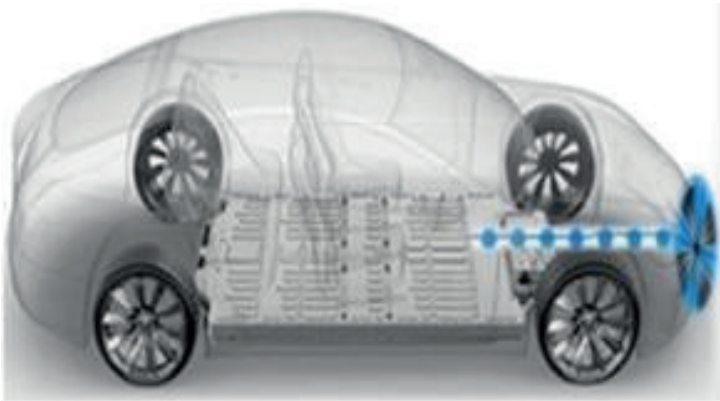
Figure 12. *PMSG Placed in the Front Ventilation Area [29]*

During the vehicle's motion, a wind flow towards the front of the vehicle occurs from the grille. Depending on the speed of the vehicle, there will be variations in the amount of air entering the vehicle. If the vehicle moves at a low speed, the airflow will be less. If the vehicle moves at a higher speed, there will be more airflow. This air will be used to generate the power needed to charge the battery in electric vehicles. Vertical Axis Wind Turbine or VAWT is used to control this incoming air. When the vehicle moves at high speed, the turbine rotates and generates power. This analysis shows that VAWT can produce 1 kW of power when the vehicle moves at a speed of 25 m/s. The efficiency of VAWT can be increased by modifying the size and shape of the blades.[30]

4) Conclusions

Electric vehicles have become popular both globally and in our country. However, one of the biggest disadvantages of electric vehicles is the issue of battery life and range. Many suggestions and solutions have been proposed worldwide to address this issue. In this project, we aimed to conduct research focusing on extending the range of electric vehicles. Through our research, we observed various studies aimed at increasing the range of electric vehicles. It was generally found that renewable energy sources were utilized to generate electricity for this purpose. Therefore, we decided that wind energy was the most suitable energy source for our project. However, we noticed a lack of extensive research on the use of wind energy and wind turbines to increase the range of electric vehicles. Consequently, we chose to conduct our research using wind energy and wind turbines. As we began our research, we first came across the idea of placing a wind turbine on the roof of the vehicle. Subsequently, we examined the working principle of the system, the wind turbine used, and its operating mechanism. Based on our research, we decided that utilizing a wind turbine and achieving a more aesthetic appearance by placing the wind turbine in the radiator area of the vehicle would be appropriate. We conducted studies on how efficient the system installed in the radiator area of the vehicle could be. As a result of our studies, we concluded that a small wind turbine could be placed behind the radiator of the vehicle, allowing for the recovery of some of the kinetic energy of the wind through the radiator's crossbars. While some of this wind is generated by external wind, the main portion is produced by the kinetic energy generated by the vehicle's movement. Since the wind turbine will be placed on the rear part of the car's radiator, it won't have any effect on the aerodynamic structure of the vehicle. Thus, we won't compromise the aerodynamic design of the car, and at the same time, we'll be able to generate electrical energy as the car moves forward. With the wind turbine installed on the vehicle, the turbine will generate power after a certain speed is reached due to the wind generated while the vehicle is moving. The electricity generated by the wind turbine during travel will continuously charge the car's battery. We believe that this system will be most efficient during long- distance journeys. This is because our vehicle may not reach high speeds in urban areas and efficient battery charging may not be possible. In contrast, during out-of-town trips, as the speed of our vehicle increases, the electrical energy generated from wind power will also increase. As a result, we will continue our journey while also potentially increasing the range of our vehicle during travel. We are continuing our research to develop this system. We will begin conducting power tests for the wind turbine we intend to place in the radiator section of the vehicles. We will continue researching and conducting tests to determine how much electrical energy the vehicle will generate at various speeds and how much contribution this energy will make to the range.

REFERENCES

[1] M.Murat Tezcan, Design and Manufacturing Aspects of a Lightweight Racing Electric Vehicle, October 2023, International Conference on Electromechanical and Energy Systems (SIELMEN).

[2] Priyanka Sharma, Piyush Dhuliya, Shailendra Singh Kathait, Sunil Semwal, Tripuresh Joshi, Mukesh Pathela Electric Vehicles (EV's): A brief review – 2022 International Conference on Advances in Computing.

[3] Zhen Zhao, Yongxin Li, Baifu Zhang, Changhong Wang, Zhangwei Yan, Qingcheng Wang, Design and Analysis of a Novel Adjustable SVAWT for Wind Energy Harvesting in New Energy Vehicle, January 2022.

[4] Srabastee Biswas, December 2023, Hybrid Cars Gain Traction As Enthusiasm Ebbs For Electric Vehicles .

[5] Tanya Shiramagond, Wei-Jen Lee, Integration of Renewable Energy into Electric Vehicle Charging Infrastructure – September 2018.

[6] Nazeeya Takkalaki, Shripad G. Desai, Rishabh Mishra, Karnika Dubey, Design and Simulation of Lithium-Ion Battery for Electric Vehicle- November 2021 International Conference on Computing Communication and Networking Technologies.

[7] R Sushmitha, K Asha, J Tejaswini, V Hemanthakumari, K Harshitha, N K Suryanarayana, Implementation of Electric Vehicles Charging Station and Battery Management System – April 2023, International Conference for Innovation in Technology (INOCON).

[8] Prof. Lavina khilnani, Future of Electrıc Vehıcle .

[9] C Jeeva, T. Porselvi, D. Karthikeyan, K. Suresh, Krithika B, Devadathan S, A Review on Electric Vehicle Adaptation: Challenges, Standards and Policy Options – December 2022 International Conference on Power, Energy, Control and Transmission Systems (ICPECTS).

[10] Benjamin Frieske, Matthias Kloetzke, Florian Mauser, Trends in vehicle concept and key technology development for hybrid and battery electric vehicles - November 2013 EVS27 International Battery, Hybrid and Fuel Cell Electric Vehicle Symposium .

[11] Elektrikli Araç Nedir Ve Elektrikli Araba Özellikleri Nelerdir: Elektrikli Araçlar Hakkinda Merak Edilen Bilgiler.

[12] José Navarrete Volvo XC100: the Swedish firm's SUV range will grow above the XC90, https://www.actualidadmotor.com/en/volvo-xc100-suv-range-swedish-firm-will-grow-on-top-of-xc90/

[13] Renault E-Tech %100 elektrikli https://www.renault.com.tr/e-tech-elektrikli/batarya.html

[14] Emir Bolat, Toyota, yeni nesil batarya https://shiftdelete.net/toyota-yeni-nesil-batarya-teknolojisi

[15] Peter Johnson, Hyundai patents an all-solid-state EV battery system in the US, https://electrek.co/2024/01/02/hyundai-patent-all-solid-state-ev-battery-system/

[16] Eric Onstad and Paul Lienert Inside's, Volkswagen's quest to develop solid-state batteries January 2024, https://www.fastcompany.com/91011260/insides-volkswagens-quest-to-develop-solid-state-batteries.

[17] Melissa Pistilli, Is Tesla Making a Graphene Battery? November 2022, https://investingnews.com/daily/tech-investing/nanoscience-investing/graphene-investing/graphene-battery-tesla/

[18] MARK VAUGHN, General Motors Invests In Lithium Iron Phosphate Batteries August 2023, https://www.autoweek.com/news/a44820249/beyond-lithium-ion-gm-invests-in-lfp-batteries/

[19] E AMRİT, Types Of Electric Vehicles https://e-amrit.niti.gov.in/types-of-electric-vehicles

[20] Tezcan, Murat, Taşer Sümeyra, Dünyada Elektrikli Araca Geçiş Senaryoları, Mühendislik Alanında Uluslararası Araştırmalar - I, Aralık 2022, Serüven Yayinevi, İzmir 2022.

[21] INTELLIPAAT Atif Khan Types of Electric Vehicles(BEV, HEV, PHEV, FCEV), April 2024, https://intellipaat.com/blog/types-of-electric-vehicles/

[22] Hassan Fathabadi, Possibility of Utilizing Wind Turbine to Recover a Portion of the Kinetic Energy Losses of a Car, September 2019, IEEE Transactions On Vehicular Technology.

[23] SCIENCEDIRECT Habib Nasser, Vehicle Dynamics Conversion into Power (Dynapower) May 2014 Univ. Savoie, SYMME, F-74000 Annecy, France.

[24] Kumarasamy Palanimuthu, Ganesh Mayilsamy , Seong Ryong Lee , Sang Yong Jung, Young Hoon Joo, Comparative analysis of maximum power extraction and control methods between PMSG and PMVG-based wind turbine systems December 2022, – ScienceDirect.

[25] ENERGY ALABAMA, The American Wind Powered Car, August 2015, https://energyalabama.org/the-american-wind-powered-car/

[26] IOP Publishing, M.Murat Tezcan, Murat Ayaz, Performance analysis of aluminum wound double fed induction generator for cost-efficient wind energy conversion systems, November 2023, Technology.

[27] Hassan Fathabadi, Novel battery/photovoltaic hybrid power source for plug-in hybrid electric vehicles, November 2017, School of Electrical and Computer Engineering, National Technical University of Athens (NTUA), Athens, Greece.

[28] LınkedIn, Josef Zankowicz, https://www.linkedin.com/posts/jzankowicz_canvassai-industrialai-ev-activity-7003022962475905025-RJqZ/

[29] Ahmet Yıldız, Beşir Dandıl, Investigation of effect of vehicle grilles on aerodynamic energy loss and drag coefficient, December 2018, Journal of Energy Systems.

Chapter 3

ROTATING MAGNETIC FIELD IN INDUCTION MOTORS

Mehmet Cihat Özgenel[1]

1 Doç. Dr.,

Induction motors work according to the rotating magnetic field principle. The electrical power in the stator winding is transferred to the rotor via the rotating magnetic field. The key to the operation of the induction motor is the rotating magnetic field. The magnetic rotating field can be obtained in practice in two ways. **One of these** is to adhesive permanent magnets in a cylinder frame and rotate the frame with another motor, as seen in Figure 1.
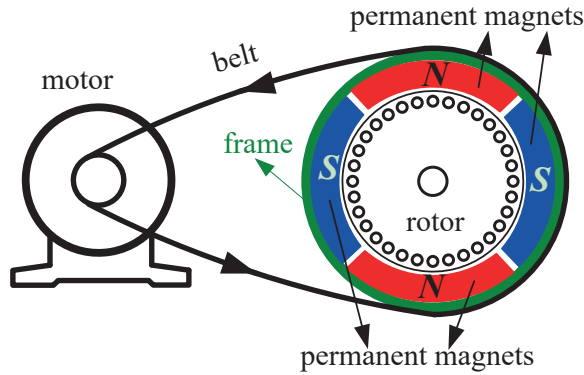
Fig. 1. Mechanically rotating magnetic field

In Figure 1 permanent magnets are glued into the frame and the frame is connected to the electric motor with a belt and pulley mechanism. When the motor rotates, the mechanical rotation movement is transferred to the frame through the belt pulley and the body begins to rotate. When the frame is rotated by the motor, the four-pole permanent magnets inside the frame also rotate. The rotation of permanent magnets creates a four-pole rotating magnetic field as seen Fig. 1.

direction of rotating magnetic field
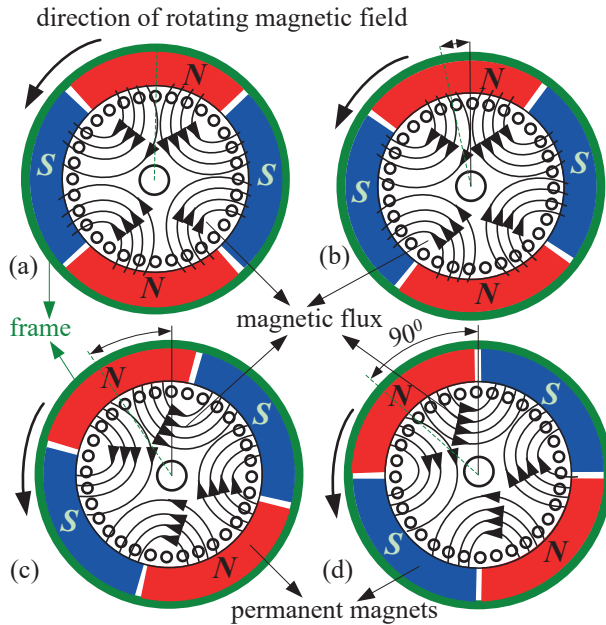
Fig. 2. Mechanically created rotating magnetic field

In Figure 2 the four-pole magnetic field moves mechanically counterclockwise. Figure 2 (a) the frame has started to rotate counterclockwise. The magnetic flux completes its circuit by leaving the N pole of the permanent magnet and reaching the S pole. When the permanent magnet magnetic field mechanically rotates counterclockwise, the magnetic flux also rotates in the same direction. In Figure 2(b) the magnetic field and magnetic flux are rotated 30 electrical degrees to the left. Similarly, in figure (c) the magnetic field and flux have rotated another 30 electric degrees. Thus, the total magnetic field and flux are rotated by 60 electrical degrees. When the frame reaches Figure (d) the magnetic field and flux have rotated 90 electrical and 45 mechanical degrees counterclockwise. As long as the electric motor continues to rotate, the magnetic field and flux will also continue to rotate. With the mechanism in Figure 1 the rotating magnetic field is obtained mechanically. Magnetic rotating field is obtained by mechanical method, but it is not used in practice. However, it is a good example to explain how the magnetic rotating field occurs.

The second of these is to create an electrically magnetic rotating field. This will be accomplished using an electromagnet. Unlike permanent magnets, the polarity and intensity of the electromagnet can be changed by varying the direction and intensity of the electric current. In fact, the stator and rotor of the induction motor are an electromagnet. To create the electromagnetic rotating field in the stator of the induction motor, it is necessary to place three-phase windings on the stator apart from 120 electrical degrees from each other and apply three-phase alternating current to the winding with a phase difference of 120 degrees between them. In induction and synchronous motors, the magnetic rotating field is obtained by this method. This method will be explained in detail on a 24-slot, four-pole real stator with three-phase winding.

Table 1. Phase polarity

steps&θ		Phase-polarity		
		Phase A	Phase B	Phase C
step1	30º	+0.5	-1	+0.5
step2	90º	+1	-0.5	-0.5
step3	150º	+0.5	+0.5	-1
step4	210º	-0.5	+1	-0.5
step5	270º	-	+	+
step6	330º	-	-	+
step1	390º	+	-	+
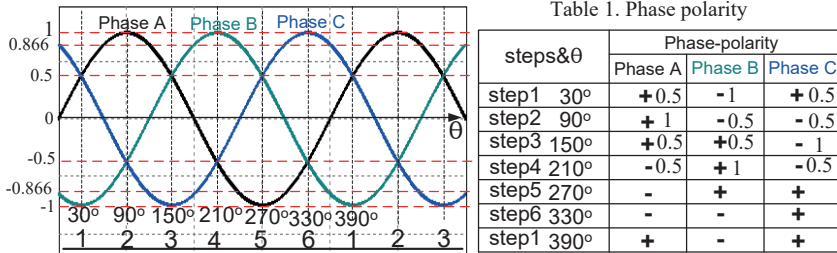
Fig. 3. Three-phase system

The three-phase system in figure 3 will be applied to the three-phase four-pole winding whose winding shape is given. In Figure 3, in step 1 (at 30 degrees), the polarity of phases A and C is positive, and phase B is negative. In the second step, after 60 degrees, the polarities of phases A and B remained the same, and phase C changed from positive to negative. In the third step, 60 degrees after the second step, the polarities of phases A and C remained the same, but phase B turned from negative to positive. Thus, the polarities of the phases change every 60 degrees. When the phase polarities change, the direction of the currents passing through the three-phase winding in the stator of the motor also changes.

Let's connect the three-phase voltage source A-phase to U-winding, B-phase to W-winding and C-phase to V-winding (Figure 4, step 1). Accordingly, the U and V windings are polarized with positive polarity, and the W winding is polarized with negative polarity, and the current

direction of U and V winding is input and the current direction of W winding is output direction. When the current directions passing through the windings are marked with arrows, polarization is seen as shown in Figure 4.
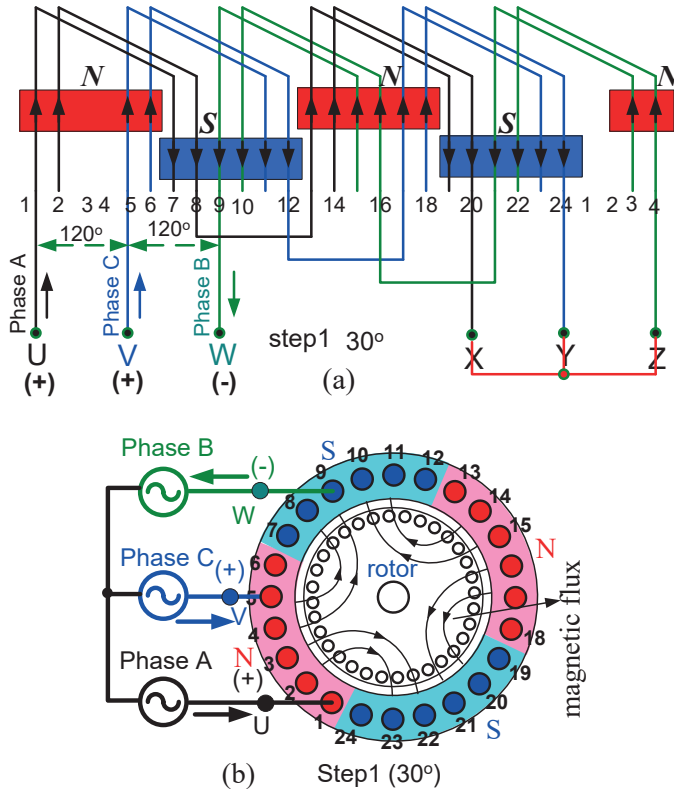
Fig. 4. Creation of electromagnetic poles according to the currents passing through windings

In Figure 4 (a, b), the currents passing through 1-6 slots, 7-12 slots, 13-18 slots and 19-24 slots created 4 magnetic poles: N, S, N, S, respectively. In other words, the currents passing through the coils in these slots have created four poles electromagnetic magnets. The occurrence of these poles can be clearly seen from the phase windings of the motor in Figure 4(a) and the cross-sectional view of the stator in (b). After 60 electrical degrees from step1, the positive polarities of phases A and B remained the same, but phase C changed from positive polarity to negative polarity

(step2). As a result, the direction of the current passing through the V winding has changed. In this case, when the direction of the currents passing through the phase windings is marked on the winding, Figure 5 (a, b) is obtained.
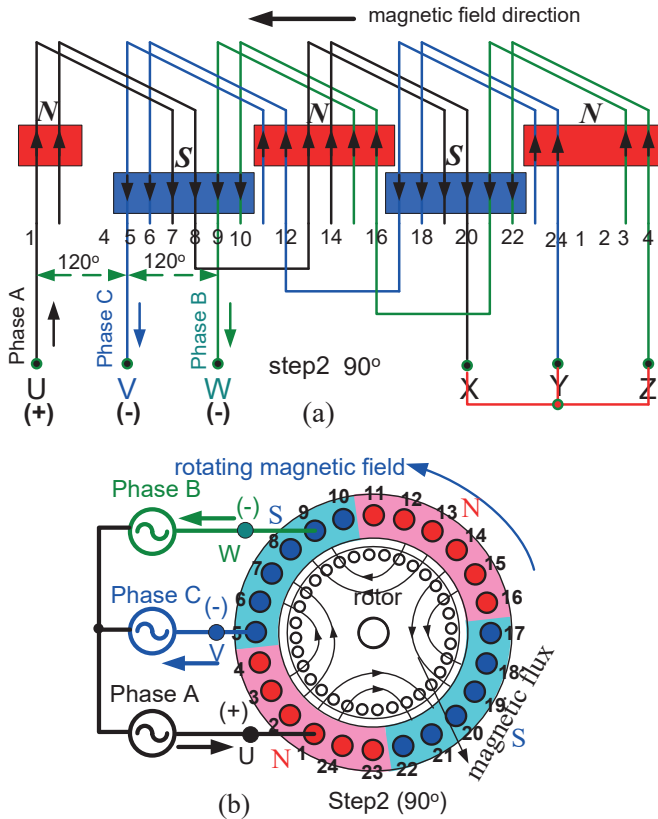
Fig. 5. Electromagnetic poles according to step2

As can be seen from Figure 5(a), the electromagnetic poles move counterclockwise by 2 slots to the left, and (b) shows that the electromagnetic poles rotate by 2 slots counterclockwise. When the alternating current reached step3, the polarities of phases A and C remained the same, and the B-Phase polarity changed from negative to positive. Thus, the direction of the W winding current has changed. When the direction of the winding current W changes, electromagnetic poles formed in the windings move two more slots to the left, as shown in

Fig. 6(a), and the electromagnetic poles rotate two more slots counterclockwise, as shown in Fig. 6(b).
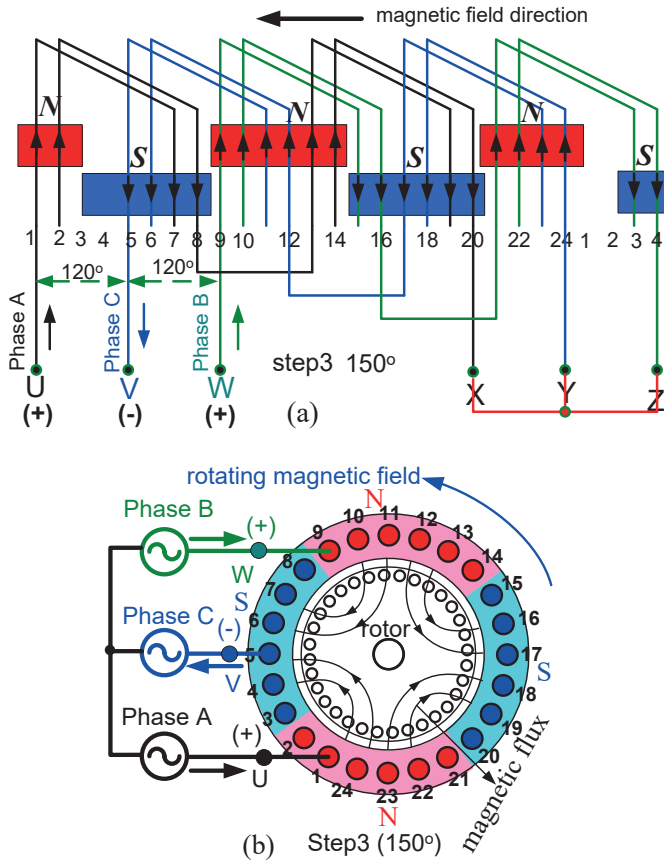
Fig. 6. Electromagnetic poles according to step3

As seen in Figure 6(a), the electromagnetic poles have shifted two slots to the left compared to the previous figure (Figure 5(a)). As seen in Figure 6(b), electromagnetic field have rotated two more slots counterclockwise compared to Figure 5(b).
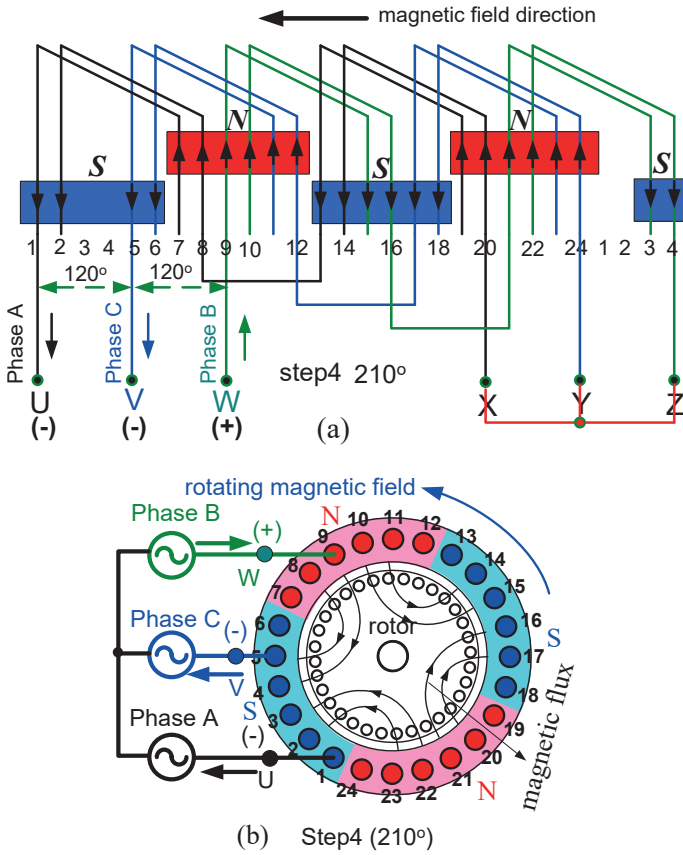
Fig. 7. Electromagnetic poles according to step4

When it comes to Step 4, the polarities of phases B and C remain the same, and the polarity of phase A has changed. Thus, the direction of the current passing through the U phase winding has changed. When the directions of the currents passing through the windings are marked again according to step 4 of Table 1, Figure 7 (a and b) is obtained. As can be seen from Figure 7(a), the electromagnetic poles have shifted two more slots to the left. Similarly, as can be seen from Fig. 7(b), the electromagnetic rotating field rotated two more slots counterclockwise. In each step from steps 1 to 4, the electromagnetic field has rotated 60 electrical degrees to the left. In total, from Fig. 4 to 7 the electromagnetic field has rotated 180 electrical degrees counterclockwise. While in Figure 4, the slots from 1 to 6 and from 13 to 18 have become the N poles, and

the slots from 7 to 12 and from 19 to 24 have become the S poles in Figure 7, the slots from1 to 6 and from 13 to 18 have become the S poles and slots from 7 to 12 and from 19 to 24 also have become N poles. Thus, from Figures 4 to 7, it is clearly seen that the magnetic field generated by the electrical manner has rotated. If we continue to mark the current directions in the windings of the motor according to the change of alternating current in Table 1, it will be seen that the electromagnetic field rotates continuously.

The speed of this rotating electromagnetic field (n_s) depends on the frequency (f) of the voltage applied to the phase windings and the pole-pair (P) of the phase windings. The speed of this rotating magnetic field created by the phase windings is called synchronous speed (n_s). The speed of the electromagnetic rotating field (ns) is expressed by the following equation [1].

$$n_s = \frac{60.f}{P} \quad (rpm) \tag{1}$$

As can be seen from expression (1), the speed of the rotating magnetic field is directly proportional to the frequency of the voltage applied to the phase windings and inversely proportional to the number of poles of the phase windings.

1-1 Magnitude of Rotating Magnetic Field

The rotating field that occurs electrically has a magnitude. Figure 8(a) illustrates the vector of the magnetic field created by the three-phase current.
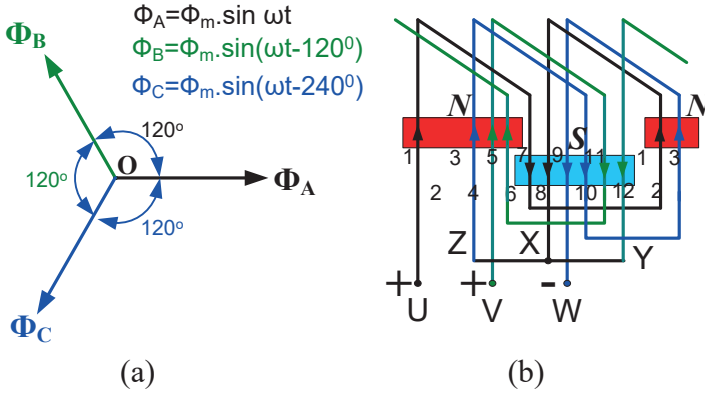
Fig. 8. Magnetic field vector produced by three-phase currents (a), 2-pole stator winding (b).

In a three-phase balanced system, the vector sum of currents and voltages is zero. This situation is clearly seen from Figure 3 and Table 1. In Figure 3, in step 1, while phase-A and phase-C are positive and have a value of 0.5, phase-C has a value of -1. In this step, the sum of the phase-values becomes zero. If we sum the values of the phases for each step, the total becomes zero. Thus, it is clearly seen that the sum of the instantaneous values of current and voltage in the three-phase balanced system is zero.

However, this is not valid for three-phase windings with 120-degree phase difference placed on the stator. In Figure 8(b), the voltage applied to the U and V phase windings is positive, while the W winding polarity is negative. While the slots numbered 1,2,3,4,5,6 are the N pole, the slots numbered 7,8,9,10,11,12 are the S pole. Thus, it can be seen that the magnetic fields created by the windings placed on the stator with a 120-degree phase difference do not cancel each other. On the contrary, the magnetic field created by each phase winding is amplifying each other. The resultant magnetic field is 1.5 times the maximum value of the magnetic field created by one phase [1, 2, 3].

Table II. Magnetic field angle

steps&θ	Phase-angle		
	Phase A	Phase B	Phase C
step0	0º	-240º	120º
step1	30º	-270º	150º
step2	90º	-330º	-210º
step3	150º	30º	-270º
step4	-210º	90º	-330º
step5	-270º	150º	30º
step6	-330º	-210º	90º
step1	30º	-270º	150º
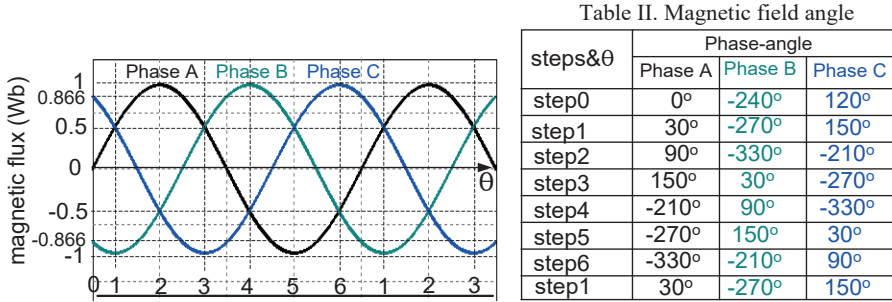
Fig. 9. Three-phase magnetic field

The amplitude of the magnetic field will be calculated according to Figure 9 and Table II. Mathematical expression of sinusoidal magnetic fluxes in Figure 9;

$$\Phi_A = \Phi_m.\sin \omega t$$

$$\Phi_B = \Phi_m.\sin(\omega t - 120^o)$$

$$\Phi_C = \Phi_m.\sin(\omega t - 240^o) \tag{2}$$

Let's calculate the amplitude of the magnetic flux created by the three phases for each step according to Figure 9 and Table II.

Step0: Instantaneous values of magnetic fluxes at this moment;

$\Phi_A = 0, \ \Phi_B = -\frac{\sqrt{3}}{2}, \ \Phi_C = \frac{\sqrt{3}}{2}$ and Φ_R is the resultant magnetic field and the vector diagram of this moment is as follows;

step0

$\Phi_A = \Phi_m.\sin 0^0$

$\Phi_B = \Phi_m.\sin(-240^0)$

$\Phi_C = \Phi_m.\sin(120^0)$

$\Phi_R = 1.5\Phi m$

OR=Φ_R=OD+DR=2OD=2DR
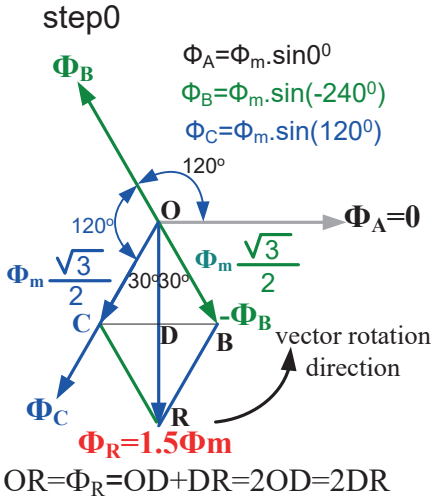
Since Φ_B has a negative sign $(-\frac{\sqrt{3}}{2})$, the Φ_B vector is drawn in the opposite direction to its own axis. Since Φ_C has a positive sign, it is drawn on its own axis. There are 60 degrees between the Φ_B and Φ_C vectors. The angle between the resultant (Φ_R) magnetic field vector and the Φ_B and Φ_C vectors is 30 degrees. According to the vector diagram; OR=Φ_R=OD+DR=2OD=2DR and OD=$OC.cos30^o = OB.cos30^o$

$$OD = \Phi_m.\frac{\sqrt{3}}{2}.cos30^o = \Phi_m.\frac{\sqrt{3}}{2}.cos30^o$$

$$\Phi_R = 0 + \Phi_m.\frac{\sqrt{3}}{2}.cos30^o + \Phi_m.\frac{\sqrt{3}}{2}.cos30^o$$

can be written.

$$\Phi_R = \Phi_A + \Phi_B + \Phi_C$$

$$\Phi_R = 0 + \Phi_m.\sin(-240^0).cos30^0 + \Phi_m.\sin(120^0).cos30^0$$

$\Phi_R = 0 + \Phi_m.\frac{\sqrt{3}}{2}.\frac{\sqrt{3}}{2} + \Phi_m.\frac{\sqrt{3}}{2}.\frac{\sqrt{3}}{2} = 2.\Phi_m\frac{3}{4} = \Phi_m.\frac{3}{2} = \mathbf{1.5\Phi_m}$ as a result, the magnetic field is 1.5 times the maximum value of the magnetic field of one phase.

Step1: Instantaneous values of magnetic fluxes at this moment;

$\Phi_A = \frac{\Phi_m}{2}$, $\Phi_B = -\Phi_m$, $\Phi_C = \frac{\Phi_m}{2}$ and Φ_R is the resultant magnetic field and the vector diagram of this moment is as follows;

step1 $\Phi_A = \Phi_m.\sin(30^0)$
$\Phi_B = \Phi_m.\sin(-270^0)$
$\Phi_C = \Phi_m.\sin(150^0)$

OR=Φ_R=OD+DE+Φ_B
=2OD+Φ_B=2DE+Φ_B
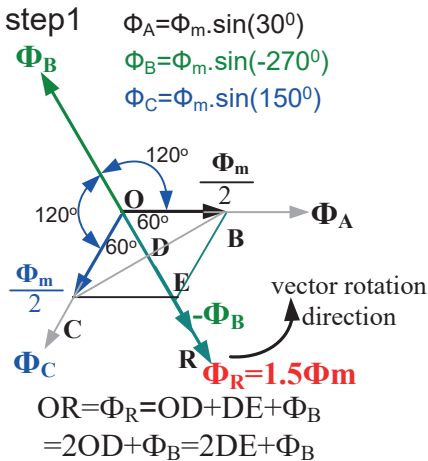
Since Φ_B has a negative sign $(-\Phi_m)$, the Φ_B vector is drawn in the opposite direction to its own axis. Since Φ_C and Φ_A have positive sign, it is drawn on its own axis. There is 60-degree between $-\Phi_B$ and Φ_A. Likewise, there is 60-degree between $-\Phi_B$ and Φ_C. The resultant magnetic field is the sum of these three vectors.

$$\Phi_R = \Phi_A + \Phi_B + \Phi_C$$

$$\Phi_R = \Phi_m.\sin(30^0).cos60^0 + \Phi_m.\sin(-270^0) + \Phi_m.\sin(30^0).cos60^0$$

$$\Phi_R = \frac{\Phi_m}{2}.\frac{1}{2} + \Phi_m + \frac{\Phi_m}{2}.\frac{1}{2} = 2.\frac{\Phi_m}{2}.\frac{1}{2} + \Phi_m = \frac{\Phi_m}{2} + \Phi_m = \mathbf{1.5\Phi_m}$$

The resultant magnetic field vector (Φ_R) has rotated 30-degree counterclockwise from step0 to step1 and it is 1.5 times one phase maximum value (Φ_m).

Step2: Instantaneous values of magnetic fluxes at this moment;

$\Phi_A = \Phi_m$, $\Phi_B = -\frac{\Phi_m}{2}$, $\Phi_C = -\frac{\Phi_m}{2}$, Φ_R is the resultant magnetic field and the vector

diagram of this moment is as follows;

step2 $\Phi_A=\Phi_m.\sin(90^0)$
$\Phi_B=\Phi_m.\sin(-330^0)$
$\Phi_C=\Phi_m.\sin(-210^0)$

vector rotation direction

$\Phi_R=1.5\Phi_m$

OR=Φ_R=OD+DE+Φ_A
=2OD+Φ_A=2DE+Φ_A
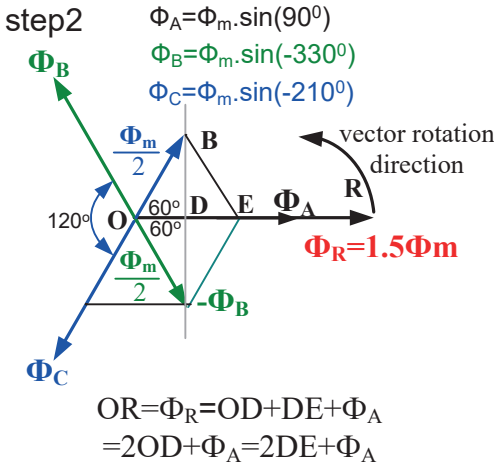
Since Φ_B and Φ_C are negative Φ_B and Φ_C vectors are drawn in the opposite direction to their own axis. There is 60-degree between $-\Phi_B$ and Φ_A. Likewise, there is 60-degree between $-\Phi_C$ and Φ_A. The resultant magnetic field is the sum of these three vectors. Φ_A is at its maximum value.

$$\Phi_R = \Phi_A + \Phi_B + \Phi_C$$

$$\Phi_R = \Phi_m + \Phi_m.\sin(-330^0).cos60^0 + \Phi_m.\sin(-210^0).cos60^0$$

$$\Phi_R = \Phi_m + \frac{\Phi_m}{2}.\frac{1}{2} + \frac{\Phi_m}{2}.\frac{1}{2} = \Phi_m + 2.\frac{\Phi_m}{2}.\frac{1}{2} = \frac{\Phi_m}{2} + \Phi_m = \mathbf{1.5\Phi_m}$$

The resultant magnetic field vector (Φ_R) has rotated 60-degree counterclockwise from step1 to step2 and it is 1.5 times one phase maximum value (Φ_m).

Step3: Instantaneous values of magnetic fluxes at this moment;

$\Phi_A = \frac{\Phi_m}{2}$, $\Phi_B = \frac{\Phi_m}{2}$, $\Phi_C = -\Phi_m$ and Φ_R is the resultant magnetic field and the vector diagram of this moment is as follows;

step3

$\Phi_R = 1.5\Phi_m$

Φ_B

$-\Phi_C$

$\Phi_A = \Phi_m.\sin($

$\Phi_B = \Phi_m.\sin($

$\Phi_C = \Phi_m.\sin($

$\dfrac{\Phi_m}{2}$

$60°$

$60°$

$120°$

Φ_A

$\dfrac{\Phi_m}{2}$

Φ_C

OR$=\Phi_R=$OD+DE+Φ_C
$=2$OD$+\Phi_C=2$DE$+\Phi_C$
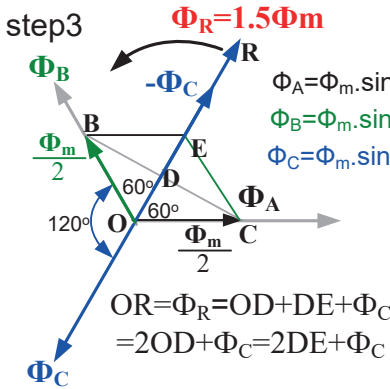
Φ_B and Φ_A are positive and Φ_C is negative signs. Φ_C vector is drawn in the opposite direction to its own axis. Φ_B and Φ_A are drawn along their own axes. There is 60-degree between $-\Phi_C$ and Φ_A. Likewise, there is 60-degree between $-\Phi_C$ and Φ_B. The resultant magnetic field is the sum of these three vectors. $-\Phi_C$ is at its maximum value.

$$\Phi_R = \Phi_A + \Phi_B + \Phi_C$$

$$\Phi_R = \Phi_m.\sin(150^0).cos60^0 + \Phi_m.\sin(30^0).cos60^0 + \Phi_m.\sin(-270^0)$$

$$\Phi_R = \frac{\Phi_m}{2}.\frac{1}{2} + \frac{\Phi_m}{2}.\frac{1}{2} + \Phi_m = \Phi_m + 2.\frac{\Phi_m}{2}.\frac{1}{2} = \frac{\Phi_m}{2} + \Phi_m = \mathbf{1.5\Phi_m}$$

The resultant magnetic field vector (Φ_R) has rotated 60-degree counterclockwise from step2 to step3 and it is 1.5 times one phase maximum value (Φ_m).

Step4: Instantaneous values of magnetic fluxes at this moment;

$\Phi_A = -\dfrac{\Phi_m}{2}$, $\Phi_B = \Phi_m$, $\Phi_C = -\dfrac{\Phi_m}{2}$ and Φ_R is the resultant magnetic field and the vector diagram of this moment is as follows;

step4

$\Phi_R = 1.5\Phi_m$

Φ_B

$-\Phi_C$

$\Phi_A = \Phi_m.\sin(-210^0)$

$\Phi_B = \Phi_m.\sin(90^0)$

$\Phi_C = \Phi_m.\sin(-330^0)$

$\dfrac{\Phi_m}{2}$

$60°$

$60°$

$-\Phi_A$

$\dfrac{\Phi_m}{2}$

Φ_A

$120°$

Φ_C

OR$=\Phi_R=$OD+DE+Φ_B
$=2$OD$+\Phi_B=2$DE$+\Phi_B$
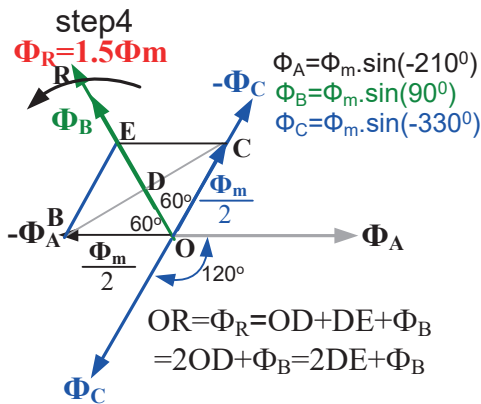
Φ_C and Φ_A are negative and Φ_B is positive signs. Φ_C and Φ_A vectors are drawn in the opposite direction to their own axes. Φ_B is drawn along its own axis. There is 60-degree between $-\Phi_C$ and Φ_B. Likewise, there is 60-degree between $-\Phi_A$ and Φ_B. The resultant magnetic field is the sum of these three vectors. Φ_B is at its maximum value.

Likewise, there is 60-degree between $-\Phi_C$ and Φ_A. The resultant magnetic field is the sum of these three vectors, which are 60 degrees apart. Φ_A is at its maximum value.

$$\Phi_R = \Phi_A + \Phi_B + \Phi_C$$

$$\Phi_R = \Phi_m.\sin(-210^0).\cos60^0 + \Phi_m.\sin(90^0) + \Phi_m.\sin(-330^0).\cos60^0$$

$$\Phi_R = \frac{\Phi_m}{2}.\frac{1}{2} + \Phi_m + \frac{\Phi_m}{2}.\frac{1}{2} = \Phi_m + 2.\frac{\Phi_m}{2}.\frac{1}{2} = \frac{\Phi_m}{2} + \Phi_m = \mathbf{1.5\Phi_m}$$

The resultant magnetic field vector (Φ_R) has rotated 60-degree counterclockwise from step3 to step4 and it is 1.5 times one phase maximum value (Φ_m).

Step5: Instantaneous values of magnetic fluxes at this moment;

$\Phi_A = -\Phi_m$, $\Phi_B = \frac{\Phi_m}{2}$, $\Phi_C = \frac{\Phi_m}{2}$ and Φ_R is the resultant magnetic field and the vector diagram of this moment is as follows;
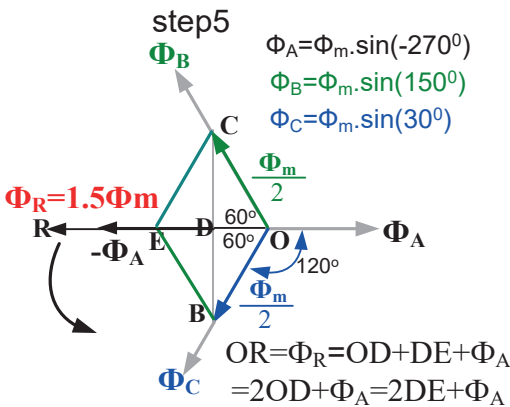
Φ_B and Φ_C are positive and Φ_A is negative signs. Φ_B and Φ_C vectors are drawn on their own axes and their values are $\frac{\Phi_m}{2}$. Φ_A is drawn along its own axis and its value is $-\Phi_m$.

There is 60-degree between Φ_C and $-\Phi_A$. Likewise, there is 60-degree between $-\Phi_A$ and Φ_B. The resultant magnetic field is the sum of these three vectors.

Likewise, there is 60-degree between $-\Phi_C$ and Φ_A. The resultant magnetic field is the sum of these three vectors, which are 60 degrees apart. Φ_A is at its maximum value.

$$\Phi_R = \Phi_A + \Phi_B + \Phi_C$$

$$\Phi_R = \Phi_m.\sin(-270^0)$$
$$+ \Phi_m.\sin(150^0).cos60^0 + \Phi_m.\sin(30^0).cos60^0$$

$$\Phi_R = \Phi_m + \frac{\Phi_m}{2}.\frac{1}{2} + \frac{\Phi_m}{2}.\frac{1}{2} = \Phi_m + 2.\frac{\Phi_m}{2}.\frac{1}{2} = \frac{\Phi_m}{2} + \Phi_m = \mathbf{\color{red}{1.5\Phi_m}}$$

The resultant magnetic field vector (Φ_R) has rotated 60-degree counterclockwise from step4 to step5 and it is 1.5 times one phase maximum value (Φ_m).

Step6: Instantaneous values of magnetic fluxes at this moment:

$\Phi_A = -\frac{\Phi_m}{2}$, $\Phi_B = -\frac{\Phi_m}{2}$, $\Phi_C = \Phi_m$ and Φ_R is the resultant magnetic field and the vector diagram of this moment is as follows;

step6 Φ_B

$\Phi_A = \Phi_m.\sin(-330^0)$
$\Phi_B = \Phi_m.\sin(-210^0)$
$\Phi_C = \Phi_m.\sin(90^0)$

$\frac{\Phi_m}{2}$ 120°

B   O Φ_A
$-\Phi_A$ 60°
D   60° $\frac{\Phi_m}{2}$
E $-\Phi_B$
Φ_C C

R
$\Phi_R = 1.5\Phi m$ vector rotation
direction
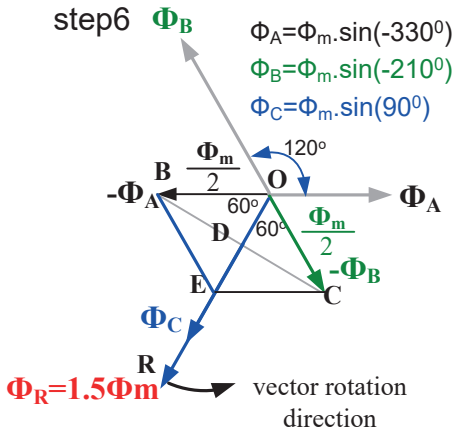
Φ_A and Φ_B are negative and Φ_C is positive signs. Φ_A and Φ_B vectors are drawn in the opposite direction of their axes and their values are $\frac{\Phi_m}{2}$.

Φ_C is drawn along its own axis and its value is Φ_m. There is 60-degree between Φ_C and $-\Phi_A$. Likewise, there is 60-degree between $-\Phi_B$ and Φ_C. The resultant magnetic field is the

sum of these three vectors.

$\Phi_R = \Phi_A + \Phi_B + \Phi_C$

$\Phi_R = \Phi_m.\sin(-330^0).\cos 60^0 + \Phi_m.\sin(-210^0).\cos 60^0 + \Phi_m.\sin(90^0)$

$\Phi_R = \frac{\Phi_m}{2}.\frac{1}{2} + \frac{\Phi_m}{2}.\frac{1}{2} + \Phi_m = 2.\frac{\Phi_m}{2}.\frac{1}{2} = \frac{\Phi_m}{2} + \Phi_m = \mathbf{1.5\Phi_m}$

The resultant magnetic field vector (Φ_R) has rotated 60-degree counterclockwise from step5 to step6 and it is 1.5 times one phase maximum value (Φ_m).
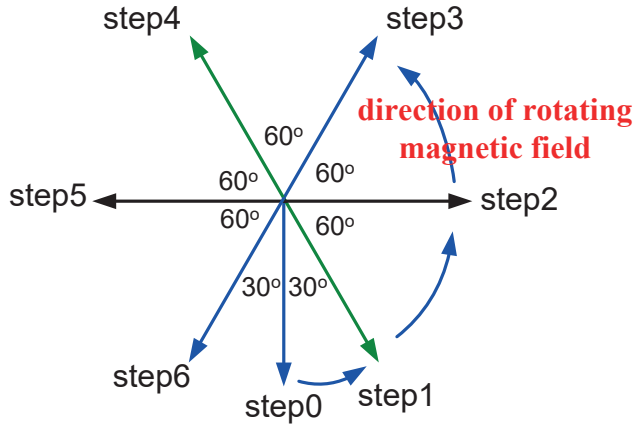
Fig. 10. Rotating magnetic field vector

Here, the movement of the magnetic field was examined at 60 degree intervals at positions 30 degrees after the initial position. Even if the inspection intervals are shorter, the result will not change, the magnetic field vector will still be 1.5 times the maximum magnetic field value of one phase.

Thus, it is seen that from step0 to step6, the magnetic field vector rotates 330 degrees counterclockwise, with its amplitude remaining constant $(1.5\Phi_m)$.

REFERENCES

[1] Fitzgerald, A. E., C. Kingsley, Jr., and S. D. Umans. Electric Machinery, 5th ed. New York: McGraw-Hill, 1990.

[2] P. C. SEN, Principles of Electric Machines and Power Electronics, Second Edition, John Wiley & Sons, 1997.

[3] Prof. Dr. Kemal Sarıoğlu, Asenkron Makinalar, Çğlayan Kitabevi yayınları, İstanbul, 1983.

THE CHARGING METHODS OF ELECTRICAL VEHICLES AND THE EFFECTS OF CHARGING STATIONS ON DISTRIBUTION GRID

Umut YILMAZ[1]

Naim Suleyman TING[2]

1 M.Sc. Student, Erzincan Binali Yildirim University, Institute of Science and Technology, Department of Electrical Electronics Engineering, umut.yilmaz@tedas.gov.tr, ORCID: 0009-0005-0605-5795.
2 Assoc. Prof. Dr., Erzincan Binali Yildirim University, Faculty of Engineering and Architecture, Department of Electrical Electronics Engineering, nsuleyman@erzincan.edu.tr, ORCID: 0000-0003-3743-0824.

1. INTRODUCTION

Nowadays, as a result of the rapid increase in population and the rapid development of technology, the increasing use of fossil fuels causes an increase in the global warming and the other environmental events. The increase in the use of fossil fuels such as diesel, gasoline and LPG is triggered by the increase in the number of vehicles. The countries are enacting laws and regulations to limit carbon and toxic gas emissions caused by the vehicle industry. Electrical vehicles offer better alternatives for people who want to use these vehicles, as they operate without the need for fossil fuels. The increased use of electrical vehicles is lead to new opportunities and technological developments. In parallel with the development of electrical vehicles, charging technology continues to develop rapidly. For this reason, large investments continue to be made on charging technology. Charging stations also increase in proportion to the increasing number of electrical vehicles. This is lead to an increase in electricity demand and, accordingly, the development of electrical grids and an increase in investments. Studies conducted around the world on the effects of electrical vehicle charging stations on the grid have been examined and are summarized below.

Wang and his friends predict that the high proliferation of electrical vehicles will have a major impact on the distribution grid. They have stated that uncontrolled charging will cause voltage and overload and technical losses will increase (Wang et al., 2012). The impact of electrical vehicles on the grid is examined in terms of load profile, power loss and voltage changes. The negative effects of the widespread use of electrical vehicles in terms of technical losses are emphasized and it is stated that at high rates of proliferation, problems such as feeder overload, voltage drop and excessive increase in technical losses occurred (Li et al., 2012). The effects of electrical vehicles on the distribution grid have been examined in Canada. He observed the load on the distribution grid, voltage status and losses. He stated that it will not have any impact in the case of Level-1 charging, but in the case of Level-2, additional investments in the distribution grid will be required (Akhavan et al., 2012).

The effects of fast charging stations, which charge electrical vehicles in less than 15 minutes, on the medium voltage grid are examined. It is modeled fast charging stations connected to the medium voltage grid with Digsilent PowerFactory software. As a result of simulations with real scenarios, it is concluded that fast charging stations do not cause much impact on the electrical grid and power transformer (Farkas et al., 2013). By modeling the real distribution grid in Finland, it is stated that the impact of electrical vehicles on the grid is not significant in terms of grid load and voltage change. It has been stated that even the high prevalence of electrical vehicles will not cause problems, and the important effect of this is that the Finnish grid is designed for the high power and energy demand due to electric heaters and stoves (Rautiainen et al, 2013).

Since the electrical buses will use more electricity, the power they will draw from the electricity grid will be more. This means that new scenarios should be created regarding the capacity and charging time of charging stations (Leou and Hung, 2017). It has been stated that high-power fast charging stations will be used due to the long charging times of electric buses used in public transportation. In this case, studies have been carried out on new problems in the electricity grid (He et al., 2020). In his study on the effects of electrical vehicle charging stations on the grid, it is stated that they will not pose a problem for now, but the situation will change due to the increase in investments in electrical vehicles (Santos et al., 2021). It has been stated that the use of electricity will increase due to the increase in the use of electrical vehicles and the increase in battery replacement stations will reduce the impact of this situation (Traini et al., 2020).

Studies have also been conducted in Turkey on the impact of the widespread use of electrical vehicle charging stations on the electricity distribution grid. Grid modeling of Trabzon province is made, charging stations are positioned in the areas where they would be needed, and their effects on the distribution grid are examined. In the modeling created with Digsilent Power Factory, no negative effects are seen that would affect the distribution system in 2025, but it is stated that the distribution system would be negatively affected in 2030 (Tan, 2023) Electrical vehicle loads created as a result of Monte Carlo simulations in the low voltage (LV) grid selected as the pivot are transferred to Digsilent PowerFactory software and as a result of load flow analysis; It has been observed that there are distribution transformer, line loading, voltage drop and grid losses. For this reason, it has been stated that electrical vehicles affect the grid and investment in the LV grid is necessary (Temiz, 2015). The eleven distribution transformers on the same distribution grid on the European side of Istanbul are examined, and the loading and voltage states of the distribution transformers are interpreted. As a result of the modeling, it is observed that there is no overloaded grid inventory and there is no voltage drop (Şen, 2019). Other thesis studies on LV grids have also reached similar results (Ünsal, 2018; Polat, 2018).

2. ELECTRICAL VEHICLES

The history of electrical vehicles, which are rapidly becoming widespread, actually dates back further than vehicles that use fossil fuels. Professor Straitingh designed a provincial electrical vehicle model in the Netherlands in 1935 (Şenlik, 2015). In the 1890s, electrical vehicles are both produced and sold in America and Europe. In fact, in the early 1990s, the number of electrical vehicles in America exceeded the number of fossil fuel vehicles. The most important problem is the range increase situation. For this reason, a hybrid structure is designed with the idea of combining electric and gasoline engines. However, between 1920 and 1960, with the decrease in gasoline prices, the development of internal

combustion engine vehicles by Charles Kettering and Henry Ford, the decrease in vehicle costs and the increase in the need for long range, intense interest in internal combustion engines increased all over the World (Kerem, 2014). Due to the rapid increase in mass production, there is no demand for electrical vehicles in the 1930s. After the 1960s, interest in electrical vehicles started again due to air pollution caused by vehicles using fossil fuels. With the oil crisis in America and European countries, interest in electrical vehicles increased rapidly. Since the 1980s, states began to give economic incentives to electrical vehicles due to their low harm to the ecological environment. With the increase in incentives, incentives for the development of charging stations designed to meet the electricity needs of electrical vehicles have begun to increase.
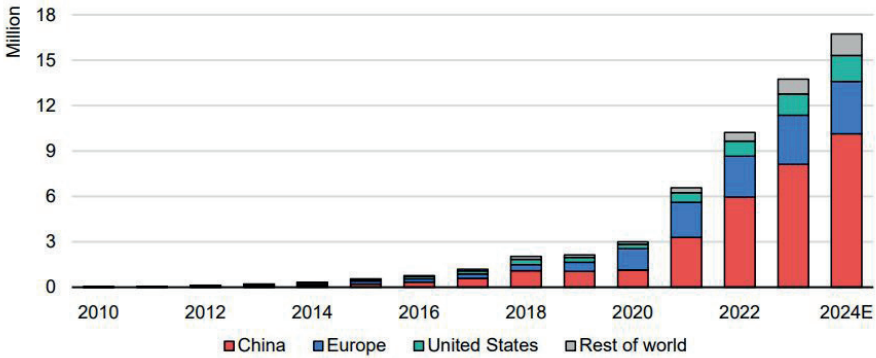
Figure 1. *Number of electrical vehicles worldwide (2024E: first quarter of 2024) (URL 1)*

As can be seen in Figure 1, the demand for electrical vehicles appears to be increasing rapidly day by day. It seems that the number of electrical vehicles worldwide will be more than 15 million in the first quarter of 2024. It is predicted that the total number of electrical vehicles worldwide will reach a minimum of 120 million and a maximum of 250 million by 2030. (URL 2)
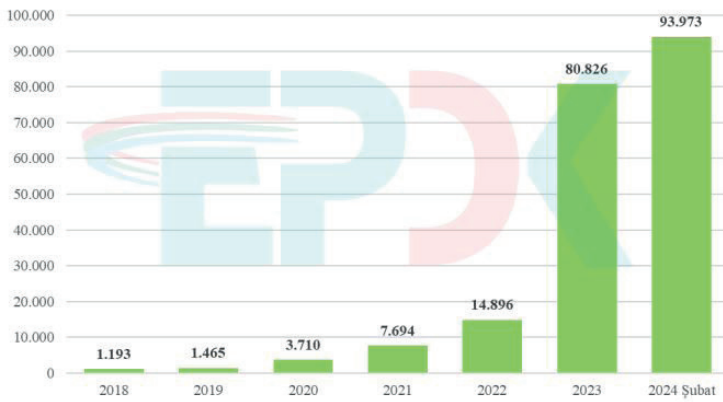
Figure 2. *Total number of electrical vehicles across Turkey (URL 3)*

As can be seen in Figure 2, there is a parallelism between Turkey and the world market. The number of electrical vehicles, which is 1,194 at the beginning of 2019, increased to 14,896 in 2022 and 80,826 in 2023. Figure 3 shows the predicted number of electrical vehicles from the study conducted by the Energy Market Regulatory Board. It is predicted that the total number of electrical vehicles in Turkey will reach a minimum of 776,362 and a maximum of 1,679,600 by 2030. Considering this increasing number of electrical vehicles, charging stations and distribution grid will need to develop in parallel.

Table 1. *Electrical vehicle projection (URL 3)*

Year	Number of Electrical Vehicles		
	Low Scenario	Medium Scenario	High Scenario
2025	202.030	269.154	361.893
2030	776.362	1.312.932	1.679.600
2035	1.779.488	3.307.577	4.214.272

3. ELECTRICAL VEHICLE CHARGING METHODS, TYPES AND STANDARDS

Today, electrical vehicles are charged in three different ways. Although the wired charging method is most commonly preferred; battery replacement and wireless charging methods are also used. The battery replacement method is preferred by those who care about the time loss of electrical vehicles while charging. In case the electrical vehicle runs out of charge, it is replaced by a full battery with an empty one at charging centres. The wireless charging method is placed on the charging surface and the vehicle is charged by electromagnetic waves generated in the electric field. It is not widely used because it is still at a technological development stage. It is especially aimed to charge vehicles while driving (Yazıcı, 2013).

Wired charging method is the most widely used method because it is reliable. In this method, the features of the charging stations are important. More detailed information on this subject will be given in the following sections. Today, these battery charging types are divided into three groups. These charging types are named Level 1, Level 2 and Level 3. Investments are being made on these specified charging types. Table 2 provides a basic comparison of Level 1, 2 and 3 charge types (Kilic, 2012*).* Level 1 charging type is used in single-phase systems and is defined as slow charging. The charging elements are mounted on the electrical vehicle in this type of charging and there is no power converter. It only serves as communication between the vehicle and the grid. Level 2 charging type has the same characteristics as Level 1. The only difference from Level 1 is that it has medium-speed charging capability. It is used in single phase systems and is mounted on the vehicle. Level 3 charging

type is also defined as fast charging. There are two types, AC and DC, as shown in Table 2. In the AC type of this charging type, three-phase systems are used for feeding, while in the DC type, a DC source obtained by rectifying the AC grid is used for feeding. While the charging elements are mounted on the vehicle in the AC type, they are not mounted on the vehicle in the DC type. (Boulanger et al., 2011; Haghbin, 2010). Therefore, in this type of charging stations, the elements required for charging are designed on the station or the vehicle, depending on whether it is AC or DC type. Additionally, different plug socket types are used in charging stations. These sockets are selected according to certain standards. For on-board chargers, the IEC 62196-2 standard is used for Europe and the SAE J1772 standard is used for the USA. For off-vehicle chargers, the IEC 62196-2 Combo standard is used for Europe and the CHAdeMO standard is used for the Far East and Japan (Kilic, 2012).

Table 2. *Types and standards of charging stations (Kilic, 2012)*

	USA	JAPAN	EU		CHINA
Single Phase / Threee Phase AC Charging	SAE J1772	SAE J1772	IEC 62196	IEC 62196-2	IEC 62196
	Level 1, 2	Level 1, 2	Level 1	Level 2, 3	Level 1, 2
	Single Phase	Single Phase	Single Phase	Single / Three Phase	Single / Three Phase
DC Fast Charging / AC-DC Combo	SAE J1772 Combo	CHAdeMO	IEC62196-3 Hybrid Combo		GB/T 20234.3
	Level 1,2	Fast Charging			Fast Charging
	DC	DC			DC
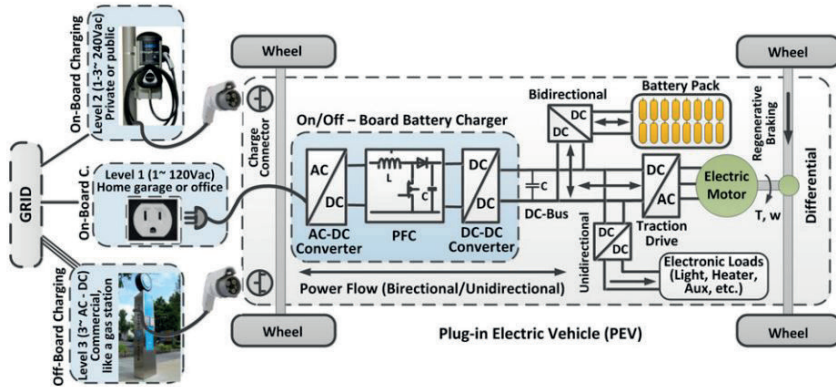
Figure 3. *On/off board charging system and power levels for electrical vehicles (Yilmaz and Krein, 2013)*

On/off board charge system are chargers called slow and fast charging, which are named according to their locations. There are two types of chargers: on-vehicle and off-vehicle chargers. In AC type systems of Level 1, Level 2

and Level 3, an on-board charger is used. Since it is small and light, it is fixed on the electrical vehicle. On-board chargers connect to 220V and 230V AC sockets and convert them into DC to charge the battery. Its advantage is that the device lasts longer because it charges slowly, and it can be charged with always available AC. Additionally, it is used without investment costs. Its disadvantage is that the charging time is long because it charges slowly. In DC type systems of Level 3, an off-vehicle charger is used. This device is a system in which electricity is transferred directly to the battery. After the AC current is converted to DC at the charging station, it is transferred directly to the vehicle battery. Therefore, it charges quickly. This provides an advantage as it is charged in a short time. Its disadvantages are that it has investment costs and battery life is shortened due to fast charging (Yilmaz and Krein, 2013). Not every charging station can be installed in every residential unit to meet the system requirements. Table 3 shows which level of charging station can be installed in which residential units (Cogen, 2010).

Table 3. *Locations of Charging Stations Type*

Settlements		Charging Station Type		
		Level 1	Level 2	Level 3
Homes	Detached Houses	√	√	-
	Apartments	√	√	-
Commercial / Business Centers	Private Properties (Offices, workplaces)	√	√	-
	Retail / Commercial (fleet and distribution services)	√	√	-
	Public Areas (Airports, Hotels, Markets, Hospitals, Shopping Malls, etc.)	√	√	√
	Government, Universities and Municipal Facilities	√	√	-
	Connection Gateways	-	√	√
	Gas Stations	-	√	√
Public Areas	Parking Areas	√	√	√
	Street	-	√	√
	Intercity Roads and Highways	-	-	√

4. ELECTRICAL VEHICLE CHARGING STATIONS

As can be seen in Figure 4, it shows that states give importance to different priorities in slow and fast charging rates. China is pioneering electrical vehicle stations. More than 85% of the world's fast chargers are located in China. 60% of slow charging stations are located in China (URL 1). There are a total of 8,229 charging stations in Turkey. The distribution of these charging stations by city is given in Figure 5. There are a total of 19,405 socket connections in

these charging stations, 12,488 of which are AC and 6,957 of which are DC sockets. The total output power of these sockets is 1,189.6 MW. With 2,165 sockets in Ankara, its proportion in the total number of sockets is 11%. 672 of the number of sockets in Ankara are located in Çankaya district. Additionally, Çankaya district is the district with the highest number of sockets in Turkey. Of the 19,405 sockets in Turkey, 53% of all sockets are sockets with 22 kW output power. This is followed by sockets with 120 kW output power with a rate of 12%. The number of electrical vehicles per AC socket is 8, and the number of electrical vehicles per DC socket is 14.4.
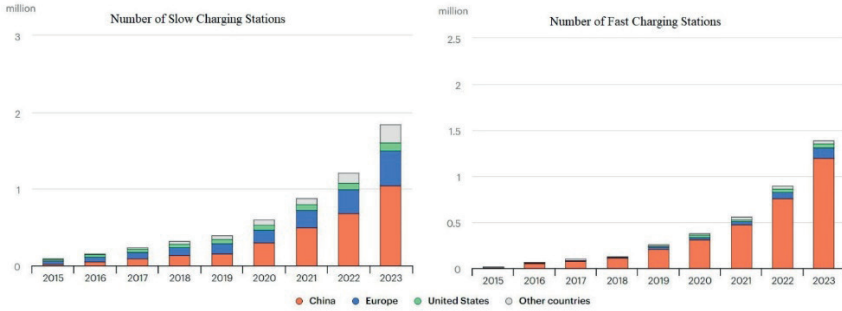
Figure 4. Number of charging stations in the world (URL 1)

Figure 5. Number of sockets on the map of Turkey (URL 4)
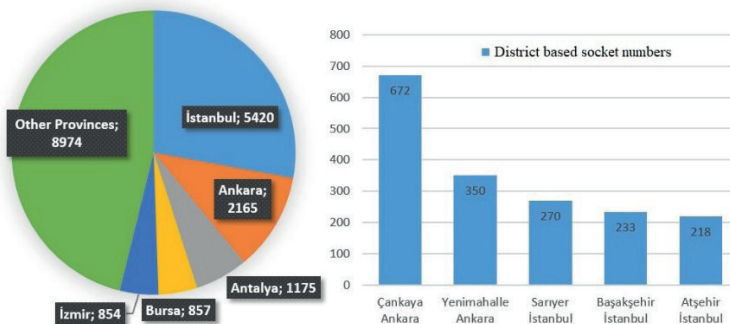
Figure 6. Province and district numbers of charging sockets (URL 4)
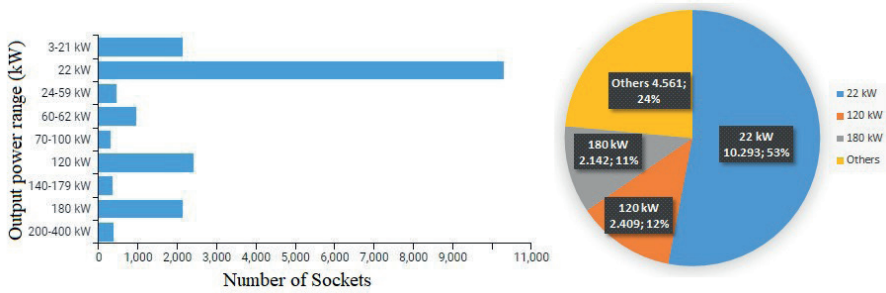
Figure 7. Numbers and ratios of charging socket power outlets (URL 4)

5. RESULTS and DISCUSSION

In this study, to examine the impact of electrical vehicle charging methods on the distribution grid, studies are conducted on sample data from Ankara. Interpretations are made on the data according to the transformer conditions on two different selected feeders. When choosing these two feeders, one is specifically chosen as urban and the other as rural. The urban area is chosen because it is densely populated and has high daily electricity demand. The rural area is chosen because the population is small and the daily demand is low. The change in the load and subscriber numbers of 20 transformers on a feeder coming out of the Distribution Center coded BAA289 located in Çankaya district, which is in the urban region of Ankara, is examined over a 5-year period. The power of the transformers on this distribution grid is high due to the dense population and electricity demand. In the 5-year period review, the average load increase is found to be 10.67%. Since the factors affecting this increase will change every year, the average of the specified years has been taken.
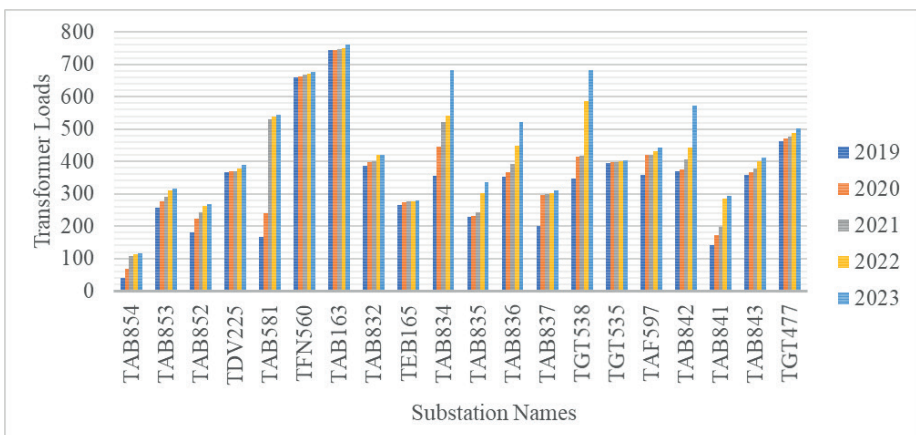
Figure 8. Transformer loads in urban areas
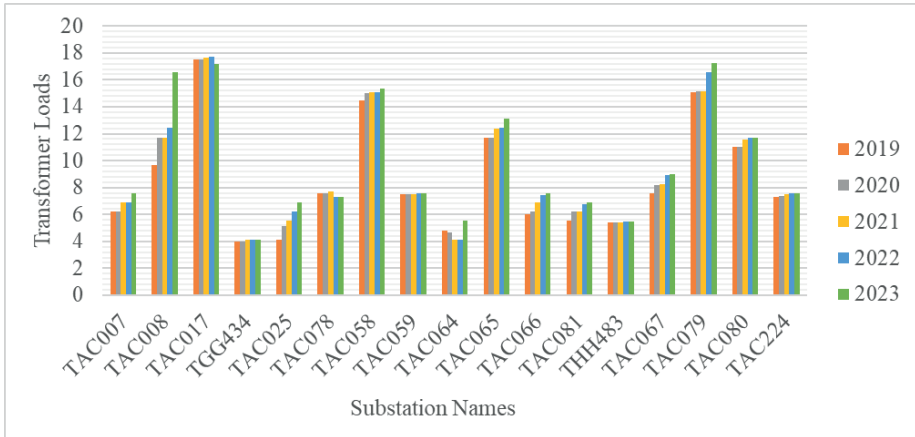
Figure 9. Transformer loads rural areas

The change in the load and subscriber numbers of 17 transformers on a feeder coming out of the Distribution Center coded BAA295 in the Nallıhan district, which is in the rural region of Ankara, is examined over a 5-year period. The power of the transformers on this distribution grid is low due to the low population and low electricity demand. In the 5-year period review, the average load increase is found to be 3.88%. Since the factors affecting this increase will change every year, the average of the specified years has been taken.

It is observed that the average occupancy rate of 20 transformers on the distribution feeder in the urban area is 42.38%. There are mostly 1000 kVA and 1600 kVA transformers on the feeder. As it can be seen in Figure 8. For the 1000 kVA transformer, it has been calculated that there is a gap of 576.2 kVA power, and that a maximum of 25 electrical vehicles can be charged instantly at 22 kW charging stations, and a maximum of 4 electrical vehicles can be charged at 120 kW charging stations. For the 1600 kVA transformer, it has been calculated that there is a gap of 921.92 kVA power, and that a maximum of 41 electrical vehicles can be charged instantly at 22kW charging stations, and a maximum of 7 electrical vehicles can be charged at 120kW charging stations. It is observed that the average occupancy rate of 17 transformers on the distribution feeder in the rural area is 18.26%. There are mostly 50 kVA and 100 kVA transformers on the feeder. Due to the low power of the transformer, it is not appropriate to use 120 kW charging stations. Therefore, calculations are made on the 22 kW charging station. In the case of a 50 kVA transformer, there is a gap with a power of 40.87 kVA, this gap can be used to charge a maximum of 1 electrical vehicle at 22 kW charging stations, and in the case of a 100 kVA transformer, there is a gap of 81.74 kVA power and this gap can be used to charge a maximum of 3 electrical vehicles at a time in charging stations with a power of 22 kW.

6. CONCLUSION

The increase in the number of electrical vehicles in distribution transformers and the consequent increase in the number of charging stations shows that the capacity of the transformers will not be sufficient. Developing technology and the development of high-power charging stations to reduce charging times will further trigger this situation. The fact that this demand will be diverted from the grid will strain the capacities of all elements used in the distribution grid, shorten their lifespan and reduce their quality. Although increasing the capacity of distribution grid elements is the first method that comes to mind to solve these problems, it is both difficult and costly. For now, the best way to prevent these problems will be to use the distribution grid very effectively and efficiently. In particular, it will be necessary to balance the distribution of high-speed charging stations among the transformers in the distribution grid. It is possible that investments in the distribution grid will increase, especially in the projections for the coming years. The location of the transformer centers to be established will be of great importance when making investments. Increasing the number of common use areas such as parks in settlements and making transformer investments in these places will yield better results. In fact, it will be necessary to build parking areas only for electrical vehicle charging stations and install transformers for this area. The biggest reasons for the increase in such investments are developing technology and increasing the power of charging stations to reduce charging time.

REFERENCES

Akhavan-Rezai, E., Shaaban, M.F., El-Saadany, E.F. and Zidan, A. (2012) "Uncoordinated charging impacts of electrical vehicles on electric distribution grids: Normal and fast charging comparison", *2012 IEEE Power and Energy Society General Meeting*, pp. 1-7.

Boulanger, A.G., Chu, A.C., Maxx S. and Waltz D.L. (2011) "Vehicle Electrification: Status and Issues", *Proceedings of the IEEE*, 99(6), 116-1138.

Cogen, J. (2010) "Report of the Alternative Fuel Vehicle Infrastructure Working Group", *Oregon State Reports*.

Farkas, C., Szűcs, G. and Prikler, L. (2013)" Grid impacts of twin EV fast charging stations placed alongside a motorway", *4th International Youth Conference on Energy (IYCE)*, pp. 1-6.

Grant, C.C. (2010) "U.S. National electrical vehicle safety standards summit, Summary Rep.," Detroit, Michigan, Nov. 2010.

Haghbin, S. (2010) "Integrated Chargers for EV's and PHEV's: Examples and New Solutions", *XIX International Conference on Electrical Machines – ICEM*.

He, Y., Liu, Z., and Song Z. (2020). "Optimal charging scheduling and management for a fast-charging battery electric bus system", *Logistics and Transportation Review*", 142, 102056.

Kerem, A. (2014). "Elektrikli Araç Teknolojisinin Gelişimi ve Gelecek Beklentileri", *Mehmet Akif Ersoy University Journal of the Institute of Science*, 1-13.

Kılıç, E. (2022). "Elektrikli araç şarj istasyonlarının enerji yönetimi", *Gazi Üniversity Institue of Science*, Ankar

Leou, R. C., and Hung, J. J. (2017). "Optimal Charging Schedule Planning and Economic Analysis for Electric Bus Charging Stations", *Energies*, 10(4), 483.

Li, H., Bai, X. and Tan, W. (2012) "Impacts of plug-in hybrid electrical vehicles charging on distribution grid and smart charging", *2012 IEEE International Conference on Power System Technology (POWERCON)*, pp. 1-5.

Liu, R., Dow, L. and Liu, E. (2011) "A Survey of PEV Impacts on Electric Utilities", *IEEE PES Innovative Smart Grid Technologies Conference*, Anaheim, CA, USA.

Polat, O. (2015) "Stochastic Simulation of Electric Vehicle Charging Loads and Its Effect on Low Voltage Distribution Network", *Master Thesis, Istanbul Technical University Institute of Science*, İstanbul.

Rautiainen, A., Mutanen, A., Repo,S., Järventausta S., Tammi P.A., Ryymin R., Helin J., Unkuri A. and Pekkinen M. (2013) "Case studies on impacts of plug-in vehicle charging load on the planning of urban electricity distribution grids", *2013 Eighth International Conference and Exhibition on Ecological Vehicles and Renewable Energies (EVER)*, pp. 1-7.

Santos, P. J., Pires, A.J. and Castro R. (2021) "The impact of charging electrical vehic-

le in electrical public substations" ***2021 IEEE 15th International Conference on Compatibility, Power Electronics and Power Engineering (CPE-POWE-RENG)***, July 14-16.

Şen, Y.R. (2019) "The model of the distribution network of electric vehicle charging stations, ***Master Thesis, Okan University Institute of Science***, İstanbul.

Şenlik, İ. (2015). "Uyuyan Devrim: Elektirikli Araçlar", ***Elektrik Mühendisliği***, 64-67.

Tan O. (2023) "Effects of Vehicle Charging Stations on Trabzon Network", ***Master Thesis, Karadeniz Technical University Institute of Science***, Trabzon.

Temiz A. (2015) "Assessment Of Impacts Of Electrical vehicles On Low Voltage Dıstrıbutıon Grids In Turkey", ***Master Thesis, Middle East Technical University Institute of Science***, Ankara.

Traini, E., Alberto, F., Bruno, G., and Lobardi, F. (2020) "Design and Simulation of a Battery Swapping System for Electrical vehicles", ***25th IEEE International Conference on Emerging Technologies and Factory Automation (EFTA)***, September 8-11.

URL 1: IEA, 'Global EV Outlook 2024', Glob. EV Outlook 2024, 2024, URL: https://www.iea.org/reports/global-ev-outlook-2024, doi: 10.1787/d394399e-en, Son Erişim Tarihi: 06.06.2024.

URL 2: Shura Enerji Dönüşüm Merkezi, 'Türkiye ulaştırma sektörünün dönüşümü : Elektrikli araçların Türkiye dağıtım şebekesine etkileri', URL: https://shura.org.tr/turkiye-ulastirma-sektorunun-donusumu-elektrikli-araclarinturkiye-dagitim-sebekesine-etkileri/, Son Erişim Tarihi: 06.06.2024.

URL 3: EPDK, "Elektrikli Araç ve Şarj Altyapısı Projeksiyonu", Nisan 2024, URL: https://www.epdk.gov.tr/Detay/Icerik/4-14379/elektrikli-arac-ve-sarj-altyapisi-projeksiyonu- , Son Erişim Tarihi: 06.06.2024

URL 4: Evcify Veri Platformu, URL: https://evcify.com/veri-platformu, Son Erişim Tarihi: 06.06.2024

Ünsal, A.B. (2018) "Integration, modeling and power flow analysis of the electric vehicle charging stations in the network", ***Master Thesis, Yildiz Technical University Institute of Science***, İstanbul.

Wang, H., Song, Q., Zhang, L., Wen, F. and Huang, J. (2012) "Load characteristics of electrical vehicles in charging and   discharging states and impacts on distribution systems", ***International Conference on Sustainable Power Generation and Supply (SUPERGEN 2012)***, pp. 1-7.

Yazıcı, V. and Özdemir, E. (2013) "Elektrikli Araç Şarj Yöntemleri", ***5. Enerji Verimliliği ve Kalitesi Sempozyumu***, 23-24 May, Kocaeli, 288-292.

Yilmaz, M. and Krein P.T. (2013) "Review of Battery Charger Topologies, Charging Power Levels, and Infrastructure for Plug-In Electric and Hybrid Vehicles", ***IEEE Trasnsactions on Power Electronics,*** 28(5), 2151-2169.

Chapter 5

A MATLAB SIMULINK BASED PERMANENT MAGNET SYNCHRONOUS GENERATOR WIND TURBINE MODEL

M.Murat TEZCAN[1]

Alperen TAŞ[2]

1 (Ph.D.), Kütahya Dumlupınar University Faculty of Engineering, Dept. of Electrical Electronics Engineering, ORCID ID: 0000-0002-5390-4527, murat.tezcan@dpu.edu.tr

2 (Bs.C.), Kütahya Dumlupınar University Faculty of Engineering, Dept. of Electrical Electronics Engineering, ORCID ID: 0009-0009-1335-4274, alperentas26@gmail.com

1) Introduction

The process of creating and operating a Permanent Magnet Synchronous Generator (PMSG) turbine in MATLAB Simulink is becoming increasingly important due to the rising interest in sustainable energy solutions. This process is driven by the need to mitigate the negative environmental impacts associated with traditional energy production methods. Fossil fuel power plants increase carbon emissions and contribute to air pollution, accelerating global warming, climate change, and adversely affecting human health. Therefore, the search for environmentally friendly energy solutions has heightened the significance of PMSG turbines.

The rise of PMSG turbines is supported by their inherently eco-friendly characteristics, making them indispensable for environmental protection and climate resilience. PMSG turbines operate without exhaust emissions, improving air quality and reducing the carbon footprint. Additionally, when utilized with renewable energy sources, they further decrease reliance on fossil fuels, creating a sustainable energy cycle.[1]

Despite the widespread adoption of PMSG turbines, they face inherent limitations, particularly operational efficiency constraints. The energy production capacity of wind turbines remains limited compared to fossil fuel plants, raising concerns for users who require continuous energy generation. This challenge is a significant barrier to the widespread adoption of PMSG turbines. Stakeholders in various industries acknowledge this obstacle and are actively engaged in multifaceted research efforts to overcome efficiency limitations.

Renewable energy sources play a crucial role in expanding the operational capabilities of PMSG turbines. Solar energy, with its limitless potential, and wind energy, harnessing the kinetic power of the atmosphere, are promising avenues for enhancing the energy reserves of PMSG turbines. Innovative solutions, such as integrating solar panels into the bodies of PMSG turbines and utilizing strategically placed low-power wind turbines to capture air flow during operation, offer significant potential to alleviate the efficiency constraints of PMSG turbines.

Advancements in battery technology also play a significant role in enhancing the suitability of PMSG turbines for long-term energy storage. Breakthroughs in lithium-ion battery design and advancements in solid-state battery technology promise higher energy densities and faster charging capabilities, addressing energy storage concerns. Lithium-ion batteries, the most widely used type, are known for their high energy densities and long lifespans. Solid-state batteries offer even higher energy densities, reduced fire risks, and faster charging times. These technological advancements enable PMSG turbines to store more energy in shorter periods, improving user experience.[2]

In addition to technological advancements in energy production, policy frameworks aimed at encouraging the adoption of PMSG turbines play a critical role in shaping the trajectory of sustainable energy production. Subsidies, tax incentives, and regulatory mandates aimed at reducing emissions and promoting clean energy usage act as catalysts for market penetration and technological innovation of PMSG turbines. Governments and international organizations provide various incentives to accelerate the adoption of PMSG turbines, guiding both manufacturers and consumers towards these turbines. These incentives include tax deductions for turbine purchases, financial support for the installation of energy storage systems, and regulations promoting the use of wind energy.

Aligned with technological advancements and policy support, consumer awareness and acceptance are integral to the transition to wind energy. Educational campaigns highlighting the environmental benefits, cost savings, and technological advancements of PMSG turbines play a crucial role in dispelling misconceptions and fostering a sustainability-conscious consumer culture. These campaigns introduce the advantages of PMSG turbines to broader audiences, increasing interest in eco-friendly and economical energy solutions. Educating consumers about the long-term cost benefits, low maintenance requirements, and positive environmental impacts of PMSG turbines accelerates their adoption.

2) In conclusion, the journey towards widespread adoption of PMSG wind turbines is characterized by a combination of technological innovation, policy intervention, and societal acceptance. As stakeholders collaborate to overcome the challenges impeding mainstream adoption of PMSG turbines, the vision of a sustainable energy production ecosystem, powered by renewable energy sources and supported by wind energy, draws closer to reality. This transformation not only provides environmental benefits but also creates positive economic and social impacts, marking a significant step towards a cleaner, more efficient, and more sustainable future.[3]The Necessity of MATLAB Modeling

MATLAB (Matrix Laboratory) is a high-level programming language and interactive environment used by MathWorks for details, technical programming, division, temperature and analysis. MATLAB offers powerful tools, especially for matrix-based programming, data analysis, graphical visualization, and engineering optimizations. Key features include ease of use, powerful extended functions, extensibility and strong graphics capability.

It has a wide range of uses in engineering and scientific fields. The scope of equations of various engineering disciplines such as electrical, electronic, mechanical, chemical and biomedical engineering is preferred for tasks such as system sections, air conditioning and data analysis.[4]

It provides a powerful platform for data analysis, visualization and aggregation programming. It can be easily accomplished with large data clusters, data visualization, consistent analysis, regression analysis, etc.

Image processing and video processing applications are widely preferred. The development of image processing systems can be easily accomplished using units such as image editing, object details, and face recognition.[5]

1.1) The Importance of MATLAB Modelling for PMSG Wind Turbine

The Permanent Magnet Synchronous Generator (PMSG) refers to a synchronous generator operated by permanent magnets. PMSGs are a type of generator used to produce electrical energy. Similar to traditional alternators, PMSGs also convert mechanical energy into electrical energy, but they have a different design and operation.

PMSGs feature a fixed array of permanent magnets in their rotor. These magnets are typically made of high-strength materials such as rare-earth elements. The presence of fixed magnets helps maintain the rotor's magnetic field, resulting in more efficient operation of the generator.[7]

One of the main advantages of PMSGs is their inherently low losses and high efficiency. This makes PMSGs a preferred option for applications that operate at continuously changing speeds, such as wind turbines. Additionally, PMSGs are known for their low maintenance requirements and longer lifespan due to fewer moving parts.
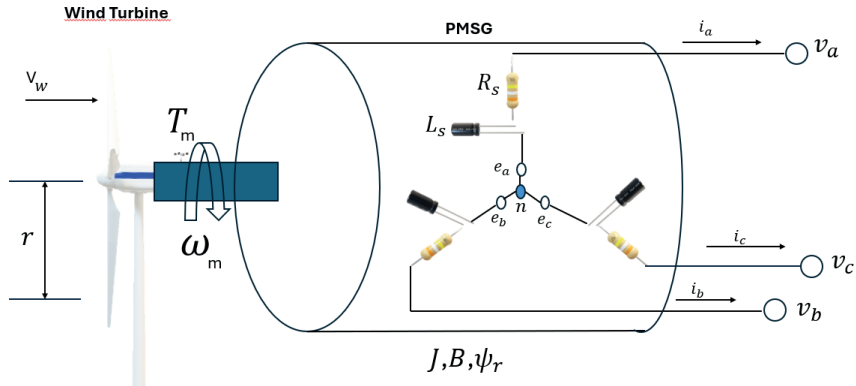
Figure 1. *A PMSG Internal Structure Example [8]*

PMSGs are widely used in renewable energy systems such as wind turbines, hydroelectric power plants, submarine power generators, and other renewable energy systems. However, they also have some disadvantages, such as high costs and the requirement for a fixed magnetic field in some applications.

Overall, PMSGs provide an effective and efficient method for generating electrical energy by harnessing the advantages of permanent magnets. Consequently, they are becoming increasingly popular in renewable energy systems.

2.2) The Structural Components of a PMSG.

This is the main component of the system. The magnetic field generator is a device that converts electrical energy into a magnetic field. It is usually connected to a power source and produces regular and repetitive magnetic field pulses using this energy. The generator can be controlled to adjust the frequency, power, and other characteristics of the magnetic field.[9]

The magnetic field generator typically contains a coil. The coil is a winding of wire through which an electric current passes to generate the magnetic field. The size, shape, and number of windings of the coil determine the power and characteristics of the generated magnetic field.These technical elements enable the PMSG system to generate, control, and apply the magnetic field. However, there may be variations between systems, and these elements may vary depending on their specifications and design.
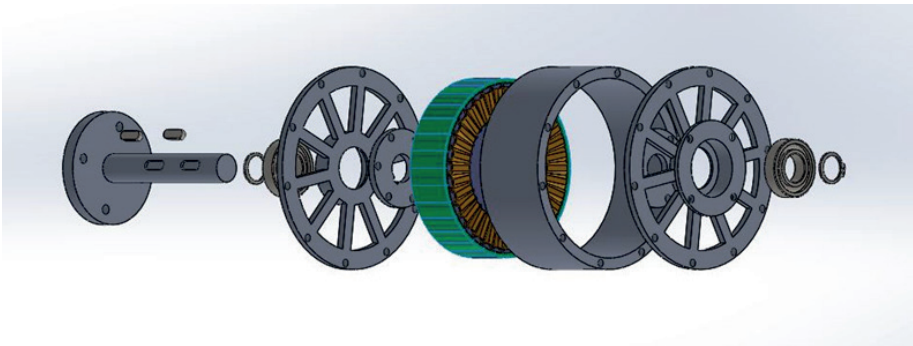
Figure 2. *PMSG Electromechanical Structure [10]*

2.2) The Significance of PMSG in MATLAB Modelling

MATLAB and Simulink are utilized to create mathematical models of PMSG (Permanent Magnet Synchronous Generator) wind turbines. Modeling the aerodynamic, mechanical, and electrical components of the turbine is crucial for accurately assessing system performance.

The efficient operation of PMSG wind turbines requires advanced control systems. MATLAB can be used to design and simulate various control algorithms (e.g., PID control, fuzzy logic, model predictive control) that ensure optimal response to changing wind speeds and load conditions. These

simulations are essential for optimizing turbine design, increasing efficiency, and identifying potential issues in advance.

MATLAB offers powerful tools for analyzing data from wind turbines and optimizing turbine performance. Analyzing data such as wind speeds, generator efficiency, and energy production enables the system to operate more efficiently. Additionally, MATLAB serves as a valuable educational and research tool for engineers and researchers working on PMSG wind turbines. Students and researchers can conduct experiments on turbine models using MATLAB. [11]

With its extensive capabilities for the design, modeling, simulation, and performance analysis of PMSG wind turbines, MATLAB's significance in this field continues to grow alongside the increasing importance of renewable energy solutions. This plays a significant role in achieving environmental sustainability goals and reducing dependence on fossil fuels [12].

2.3) The Stages Of Creating The MATLAB Model For PMSG

The first step involves defining the PMSG system and setting the modeling objectives. This stage clarifies which features of the system need to be modeled and the intended use of the model. The development of the mathematical model involves formulating the mathematical equations for the PMSG model in MATLAB. These equations represent the electrical, mechanical, and aerodynamic characteristics of the PMSG and are typically in the form of differential equations or transfer functions.

The simulation parameters for the MATLAB model are defined based on the physical properties of the PMSG and the simulation objectives. These parameters include turbine dimensions, wind speed profiles, generator characteristics, and control strategies. Using the mathematical model and simulation parameters, a code is developed in MATLAB. This code is a program that simulates the behavior of the PMSG and enables the performance of the desired analyses.[13]

The created MATLAB model is then simulated and analyzed. During this stage, the system's performance is evaluated under different operating conditions, optimizations are performed, and the results are visualized. The MATLAB model is validated by comparing it with real-world data and refined if necessary. This step ensures that the model can produce accurate results under real-world conditions.

Figure 3. *PMSG Based Wind Energy Conversion System Block Diagram [14]*

2.4) The PMSG Wind Turbine Model in Simulink

The model in the photograph simulates the interaction between a wind turbine system and a permanent magnet synchronous machine (PMSM). Such a system is typically used to convert wind energy into electrical energy.

Figure 4. *PMSG Based Wind Energy Conversion System Model in MATLAB Simulink [15]*

2.5) General Structure and Components of Modelled System

PowerGUI is a block set used for modeling and simulation of power systems in the Simulink environment. These blocks are employed in the analysis and design of electrical energy systems. PowerGUI encompasses various blocks for modeling both alternating current (AC) and direct current (DC) systems [16].

Figure 5. *PowerGUI Block*

The Constant and Slider Gain blocks are fundamental blocks used in Simulink and are frequently employed in the modeling process. The Constant block represents a constant number or value. It is used to represent a specific constant value in the model. For example, it can be used to specify a constant voltage or a reference value. On the other hand, the Slider Gain block provides a slider interface for adjusting a continuous value. This block is used to adjust or change a specific parameter during the operation of the model. For instance, it can be utilized to examine or optimize the behavior of the system during a simulation. Both blocks enhance the flexibility of the model and provide users with more control over the dynamic behavior.

Figure 6. *Constant and Slider Gain Blocks*

The Wind Turbine block is a key component in Simulink models used for simulating wind energy conversion systems. It represents the mechanical and electrical behavior of a wind turbine system within a simulation environment. This block typically includes parameters such as wind speed, turbine rotor characteristics, generator specifications, and control strategies. By incorporating these parameters, the Wind Turbine block allows engineers to analyze the performance of wind turbines under various operating conditions and environmental factors.
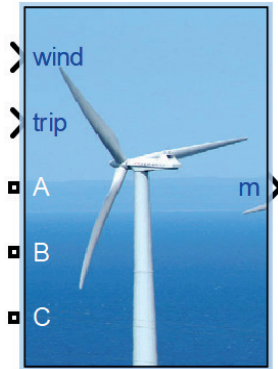
Figure 7. *Wind Turbine Block*

The Series RL Branch block is a fundamental component used for modeling electrical circuits, particularly in power system analysis, within Simulink. It represents the series connection of a resistor (R) and an inductor (L), which are commonly found in various electrical circuits. This block enables users to simulate the behavior of series RL circuits prevalent in applications such as electrical distribution networks, transmission lines, and passive filters. By specifying the resistance and inductance values, users can accurately model the impedance characteristics and transient response of series RL branches within a larger electrical system.
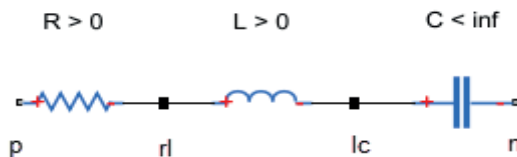
Figure 8. *Series RL Branch Block*

The Universal Bridge block is a versatile component utilized in Simulink for modeling electrical circuits, particularly in the context of bridge circuits commonly used in instrumentation and measurement applications. This block represents a generalized bridge circuit configuration, encompassing various bridge topologies such as Wheatstone, Kelvin, Maxwell, and others. By incorporating resistive, capacitive, and inductive elements, along with adjustable parameters, the Universal Bridge block allows users to simulate a wide range of bridge circuits with different configurations and operating conditions.
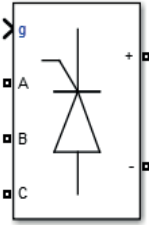
Figure 9. *Universal Bridge block*

The Three-Phase V-I Measurement Block is a fundamental component used in electrical power systems modeling within Simulink. It allows for the measurement and analysis of voltage and current signals in three-phase systems. This block enables users to monitor and record the instantaneous values of voltage and current across each phase of the system, providing essential data for various analyzes such as power flow, fault detection, and system stability assessment.
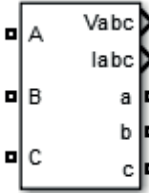
Figure 10. *Three-Phase V-I Measurement Block*

The Permanent Magnet Synchronous Machine (PMSM) Block is a key component used in Simulink for modeling and simulating the behavior of permanent magnet synchronous machines in electrical systems. This block represents the dynamic characteristics and operational principles of PMSMs, which are widely utilized in various applications such as electric vehicles, industrial machinery, and renewable energy systems.
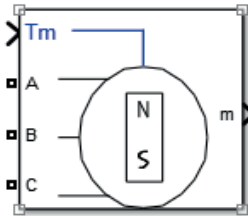
Figure 11. *Permanent Magnet Synchronous Machine*

Scope Blocks are one of the visualization tools in Simulink, used to visually monitor the dynamic behavior of the model. These blocks graphically represent the time evolution of signals at various points in the model, allowing

users to observe the changes in these signals during simulation. They provide the opportunity to monitor the variation of signals during simulation. Users can utilize Scope Blocks to analyze the behavior of the model, evaluate system performance, and visually track the design process. Additionally, these blocks can be used to visually report and sha3re simulation results. In summary, Scope Blocks provide a powerful tool for monitoring and analyzing various signals in Simulink models.[18]
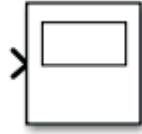
Figure 12. *Scope Block*

2.6) Operating Principle of PMSG Based Wind Energy Conversion System

In the utilized wind turbine system, a small wind turbine model has been considered. This model has been selected as a low-power wind turbine, especially since it will be used for electric vehicles. Choosing a low-power turbine ensures that the energy needs are met more efficiently and that the system is more compact and portable. For the wind turbine to operate efficiently, it is crucial to carefully monitor and optimize specific parameters such as wind speed and pitch angle.

Wind speed directly affects the amount of energy the turbine can produce, while the pitch angle ensures the efficiency of energy production and the longevity of the turbine. These two key parameters play a critical role in determining the overall performance of the turbine. Moreover, precise adjustment of these parameters allows the system to perform optimally under various weather conditions. The correct selection and integration of all components and their specific values lused in the system increase the overall efficiency and reliability of the system. Below are the specific values of the components used in the system detailed.[17]

A small yet powerful wind turbine has been considered for use in the system. These turbines are typically employed in homes, small businesses, or for specific appliances. In the established MATLAB system, a 10 kW wind turbine has been examined.

Battery capacity is determined based on energy storage requirements and the system's operating duration. Typically, a backup duration of 4-6 hours is targeted for a wind turbine system. For a 10 kW wind turbine, a 4-hour backup duration is considered, leading to the results shown in the table below. The values of conversion components are equally crucial in the system.

Conversion components include inverters and converters, which convert the AC power generated by the wind turbine into suitable power for the battery.

Connecting the energy generated by wind turbines to the electrical grid requires the use of synchronous generators. The power of these generators should be selected according to the power of the wind turbine.

Component	Specification	Capacity	Efficiency
Wind Turbine	Nominal Capacity	10 kW	-
Battery System	Storage Capacity (4 hours backup time)	40 kWh	-
AC/DC Inverter	Nominal Capacity	10 kW	%95
Power Converter	Nominal Capacity	10 kW	%95
Synchronous Generator	Nominal Capacity	10 kW	%96-%98

Table 1. *PMSG Based Wind Energy Conversion System Components Specifications*

3) Analysis of the Graph Based MATLAB PMSG Model

Using a 10 kW wind turbine, integrated with a 40 kWh capacity battery system, inverters, and power converters with 95% efficiency, along with a synchronous generator with 96-98% efficiency, ensures maximum performance and energy efficiency. The correct selection and optimization of these components enable the effective conversion and storage of small-scale wind energy into electrical energy.[20]

The provided graph shows time domain simulations from a MATLAB model of a Permanent Magnet Synchronous Generator (PMSG) driven by a wind turbine. The chart consists of two groups of waveforms.
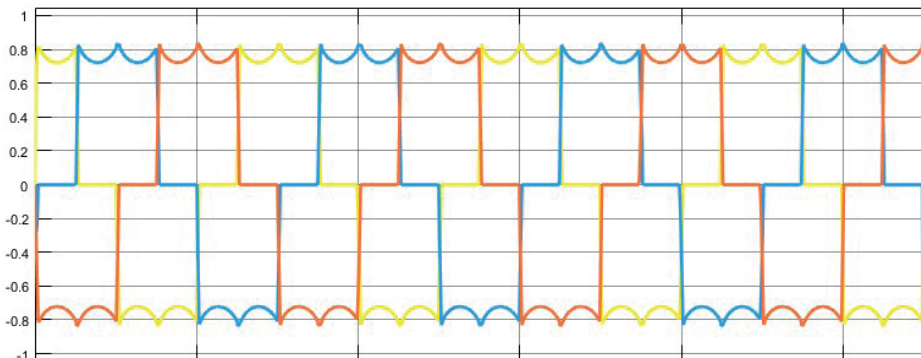
Figure 13. *DC And AC Output Voltages of PMSG*

The square waveforms on Figure 13, likely represent the voltage generated by the wind turbine and subsequently converted to direct current (DC) by a rectifier. The sinusoidal components represent alternating current (AC) voltage generated by the inverter, which is then supplied to the grid or load system. The occurrence of positive and negative maximum voltage levels indicates the conversion of turbine output voltage to AC voltage through the inverter. This synchronization with the grid is crucial for grid integration. The output frequency of the inverter is typically fixed (e.g., 50 Hz or 60 Hz) and must synchronize with the grid frequency.

Distortions and harmonics on the waveform can indicate the effects of the inverter's switching frequency. The sinusoidal and trapezoidal current waveforms on the lower graph may represent the current supplied by the wind turbine inverter to the load or grid. Sinusoidal components ideally represent pure AC current, while trapezoidal or harmonic-containing components indicate harmonic distortion from the inverter. Current levels vary depending on the power generated by the turbine and the demand from the load or grid. For a 10 kW turbine, these currents will exhibit significant magnitudes. Phase shifts between current and voltage waveforms determine the system's power factor, affecting reactive power components and energy efficiency. Harmonics present in both voltage and current waveforms can affect power quality. Harmonic analysis is crucial for evaluating inverter performance and energy efficiency. High harmonics can increase heat losses and have adverse effects on equipment.

Active power ($P = V \times I \times \cos(\theta)$), reactive power ($Q = V \times I \times \sin(\theta)$), and apparent power ($S = V \times I$) can be calculated using voltage and current waveforms. These calculations can verify the power produced by a 10 kW turbine.Efficiency of wind turbine, rectifier, and inverter systems can be analyzed through these waveforms. Sinusoidal waveforms with low harmonic content signify higher system efficiency and lower losses.

Analyzing these graphs provides valuable insights into the performance and efficiency of a 10 kW wind turbine system. Proper interpretation of voltage and current waveforms can optimize system design and operation. Considerations regarding harmonics and power quality during grid integration of wind turbine-generated power can also be identified through this analysis.

3.1) Transferring The Generated Power To The Grid
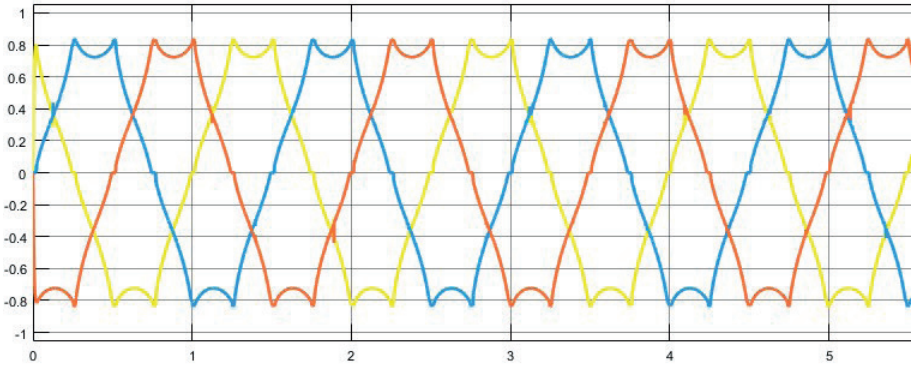
Figure 14. *Transferring The Generated Power To The Grid*

Figure 14 can be used to analyze the power generated by the wind turbine and the power transferred to the grid or load system. Below is a detailed analysis of the waveforms seen in this graph, which represent voltages for a three-phase system. In three-phase systems, waveforms have a 120-degree phase difference between them.

Each waveform is in a smooth sinusoidal form, with amplitudes and phases shifted relative to each other, as expected in a three-phase system. The 120-degree phase shift between each phase demonstrates ideal three-phase sinusoidal waveforms.

The amplitude and frequency of voltage waveforms represent the magnitude and frequency of the electricity generated by the turbine. In three-phase wind turbines, voltage amplitude and frequency are typically constant and must be compatible with the grid. Minor irregularities or distortions in waveforms can provide information about harmonic content. Low harmonics indicate high power quality.

The amplitude and frequency of current waveforms illustrate how the power generated by the turbine is utilized by the load or grid. Current amplitude represents the actual power generated by the turbine. Phase shift between current and voltage waveforms provides information about power factor, which is used in calculating reactive and active power components.

Active power is calculated as the average of the product of voltage and current waveforms, expressed in three-phase systems as $P = \sqrt{3} \times V_{line} \times I_{line} \times \cos(\phi)$. Reactive power is calculated using the formula $Q = \sqrt{3} \times V_{line} \times I_{line} \times \sin(\phi)$. The phase shift between current and voltage waveforms determines the reactive power component. A smaller phase difference results in a lower reactive power

component. Apparent power is calculated as $S = \sqrt{3} \times V_{line} \times I_{line}$, representing the total power capacity of the system.

Harmonics observed in waveforms are significant factors affecting power quality. High harmonics can lead to energy losses and negative effects on equipment. Harmonic analysis is crucial for improving power quality and using harmonic filters. Power factor ($\cos(\phi)$) indicates how efficiently the system operates. A high power factor demonstrates efficient utilization of active power. Minimizing waveform distortions enhances system efficiency and reduces energy losses.

Analyzing these graphs provides comprehensive insights into the performance and efficiency of a 10 kW wind turbine system. Accurate analysis of voltage and current waveforms in three-phase systems is critical for optimizing power generation systems and improving energy efficiency. In an academic paper, such analysis provides valuable data for the design and operation of wind turbine systems. Analysis of harmonics and power factor can be utilized to enhance overall system performance and energy efficiency.

3.2) PMSG Value Chart

The graph provided below consists of three sub-graphs, each representing different operational parameters of the Permanent Magnet Synchronous Generator (PMSG) within the MATLAB Simulink model. These parameters are rotor speed, electromagnetic torque and stator current.

3.2.1) Rotor Speed

Figure 15 shows the rotor speed of the PMSG over a period of 10 seconds. The rotor speed rapidly increases from 0 rad/s and stabilizes around 85 rad/s. The curve follows an exponential growth pattern initially and then levels off, indicating that the rotor reaches a steady-state speed. This behavior suggests that the PMSG accelerates quickly due to the mechanical input from the wind turbine and reaches its nominal operating speed. The stabilization of the speed indicates a balance between the mechanical input power and the electrical load, signifying steady-state operation.

Figure 15. *Rotor speed of the PMSG over a period of 10 seconds*

3.2.2) Electromagnetic Torque

Figure 16   illustrates the electromagnetic torque generated by the Permanent Magnet Synchronous Generator (PMSG). Initially, the torque reaches a peak of approximately 0.4 N*m before swiftly declining to around -0.6 N*m. Subsequently, the torque stabilizes at this negative value throughout the remainder of the simulation. The initial peak in torque corresponds to the rotor's acceleration phase, where greater torque is necessary to overcome inertia and friction. The presence of negative torque in steady-state signifies that the generator is supplying power to the load. In generator operation, electromagnetic torque typically exhibits a negative value as it opposes mechanical input torque. The stabilization of torque suggests that the system has achieved a steady-state condition wherein mechanical input and electrical output are in equilibrium.

Figure 16. *Electromagnetic torque generated by the Permanent Magnet Synchronous Generator (PMSG)*

3.2.3) Stator Current

Figure 17. represents the one phase stator current of PMSG. The stator current shows an initial transient spike and then gradually stabilizes. The current remains relatively constant after the initial transient, with some ripple. The initial spike in current is due to the inrush current when the generator starts and begins to build up magnetic fields within the stator windings. The gradual stabilization indicates that the generator is transitioning from startup to steady-state operation. The small ripples in the steady-state current are typical and can be attributed to the PWM control of the inverter and the harmonics generated by the switching devices.
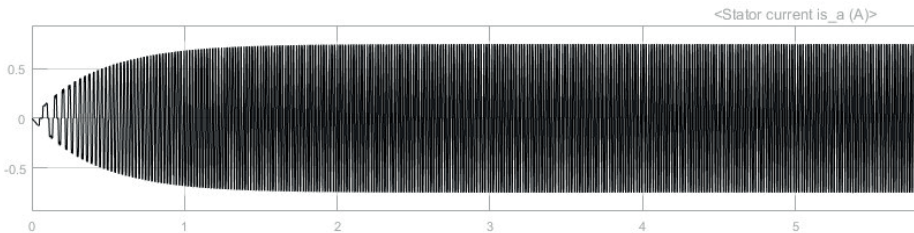
Figure 17. *One Phase Stator current of PMSG*

This graph, created in MATLAB, is likely an output from a Permanent Magnet Synchronous Generator (PMSG) model. For accurate interpretation, axis labels and graph annotations are necessary. However, based on the provided data, a general evaluation can be made.

4) Conclusions

The range issue of electric vehicles remains a significant factor limiting their widespread use. Although various solutions have been proposed to address this problem, finding a practical and effective solution for the daily use of electric vehicles remains a crucial necessity. In this context, proposed a system powered by wind energy. The recovery of kinetic energy generated during the motion of electric vehicles and its conversion into electrical energy presents a potential solution for increasing the vehicle's range.

This study also indicates that wind energy is a suitable source for extending the range of electric vehicles. In this regard, a wind turbine installed in the radiator area of the vehicle allows for the recovery of kinetic energy and the generation of electricity. However, it should be noted that research on this system is still limited, and further investigation is required.

Mathematical modeling and simulations serve as important tools for evaluating the efficiency of the proposed system's wind turbine. Simulations conducted using MATLAB Simulink help determine how much electrical energy can be generated at different vehicle speeds and how this energy can contribute to extending the vehicle's range. These simulation results provide valuable insights into the design and operation of the system, aiding in its optimization.

Proposed system operates most efficiently during long-distance travels. While the effectiveness of the wind turbine may be limited during city driving due to lower speeds and frequent stops, it becomes more efficient during highway driving as vehicle speed increases, resulting in higher electricity generation. This potential increase in range throughout the journey is noteworthy.

In conclusion, a wind energy-powered system offers a promising approach to addressing the range issue of electric vehicles or renewable energy conversion systems. Future research will focus on further developing and optimizing this system through power testing, simulations, and experimental studies. This work contributes to the advancement of electric vehicles towards a sustainable future.

REFERENCES

[1] Barton, J. P., & Infield, D. G. (2004). Energy storage and its use with intermittent renewable energy. IEEE Transactions on Energy Conversion, 19(2), 441-448.

[2] Carroll, J., McDonald, A., & McMillan, D. (2016). Reliability comparison of wind turbines with DFIG and PMSG drive trains. IEEE Transactions on Energy Conversion, 31(2), 587-594.

[3] Blaabjerg, F., & Ma, K. (2013). Future on power electronics for wind turbine systems. IEEE Journal of Emerging and Selected Topics in Power Electronics, 1(3), 139-15

[4] Hahn, B., & Valentine, D. T. (2016). Essential MATLAB for Engineers and Scientists. Academic Press.

[5] Gonzalez, R. C., & Woods, R. E. (2008). Digital Image Processing Using MATLAB. Gatesmark Publishing.

[6] 9series Inc. (2023, February 28). What is MATLAB? Medium. Retrieved June 14, 2024.

[7] Junge, B., De Doncker, R. W., & Van den Bossche, P. (2010). Analysis and design of permanent magnet synchronous generator for high-speed applications. IEEE Transactions on Magnetics, 46(6), 2152-2155. doi:10.1109/TMAG.2010.2042401

[8] Ciornei, F.; Ledesma-Alonso, R.; Nuño, E. Phase Voltage-Oriented Control of a PMSG Wind Generator for Unity Power Factor Correction. Energies 2020, 13, 5693.

[9] Doe J.(Year). "Title of the Magnetic Field Generator Device." Journal/Conference Name, Volume(Issue), Page Range.

[10] Tezcan, M. M. (2020). Performance Analysis of Inner Rotor and Outer Rotor PMSMs for Electric Vehicle Traction Systems. Journal of Polytechnic, 23(4)

[11] Yazdani, A., & Iravani, R. (2010). "Voltage-Sourced Converters in Power Systems: Modeling, Control, and Applications." IEEE Press/Wiley. DOI: 10.1002/9780470551574

[12] Tezcan, M. M. (2019). Performance Analysis Of Inner Rotor And Outer Rotor PMSMs For Electric Vehicle Traction Systems. International Scientific And Vocational Studies Journal, 3(2), pp.51 - 55.

[13] Gole, A. M., Keri, A., & Palejwala, S. (2011). "Modeling of Permanent Magnet Synchronous Generators for Transient Stability Studies." IEEE Transactions on Power Systems, 26(2), 879-886. DOI: 10.1109/TPWRS.2010.2052075

[14] IOP Publishing, M.Murat Tezcan, Murat Ayaz, Performance analysis of aluminum wound double fed induction generator for cost-efficient wind energy conversion systems, November 2023, Technology

[15] Urban Scholl PMSG Wind Turbine Model in Simulink | Permanent Magnet Synchronous Generator in Simulink Simulation.

[16] MATLAB Kütahya D.P.U. Electrical and Electronics Engineering Dept. Licence.

[17] Brown, C., & Wilson, D. (2020). Design considerations for integrating small wind turbines into electric vehicle charging systems. Renewable Energy Journal, 8(3), 112-125.

Chapter 6

ANALYSIS OF GRID-CONNECTED PHOTOVOLTAIC SYSTEMS

Süleyman ADAK[1]

1 [1]Dr.Öğr.Üyesi, Mardin Artuklu University, Vocational School, Department of Electricity and Energy, suleymanadak@artuklu.edu.tr, ORCID: 0000-0003-1436-2830.

1. INTRODUCTION

Increasing energy demand and environmental concerns have heightened interest in renewable energy sources today. In this context, photovoltaic (PV) systems are significant technologies that convert sunlight into electricity, providing a sustainable energy source. Grid-connected PV systems are integrated with the electrical grid, transmitting generated electricity into the grid. Analyzing these systems is crucial to understand their performance, enhance efficiency, and ensure reliability. The aim of this study is to present a detailed analysis of grid-connected PV systems. In this context, the study will examine system components, operational principles, and performance evaluation methods, deriving conclusions through necessary simulations. Additionally, it will address the economic and environmental benefits crucial for promoting widespread adoption of solar-powered systems. Fig. 1. shows the working principle of a grid-tied photovoltaic system.
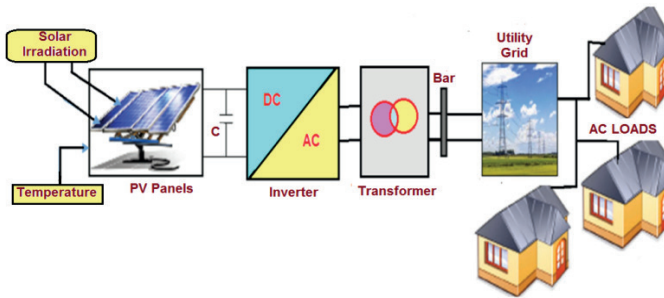
Şekil 1. Principle diagram of grid-connected PV system

Matlab/Simulink is a powerful tool for the analysis of PV systems. This platform enables the simulation of various aspects of PV systems, ranging from modeling solar panel characteristics to inverter control strategies. Solar energy is an environmentally friendly, sustainable, and widely available energy source. PV systems are technologies that convert sunlight into electricity and are increasingly being adopted. The purpose of this paper is to analyze grid-connected photovoltaic systems. Grid-connected systems operate connected to the electrical grid, either feeding excess energy into the grid or drawing energy from it. The analysis of these systems is crucial from both technical and economic perspectives. Technically, it involves examining the system's performance, efficiency, and reliability. Economically, factors such as investment costs, payback periods, and financial returns are evaluated.

2. ANALYSIS OF GRID CONNECTED PV SYSTEM

Grid-connected photovoltaic power systems consist of PV panels that convert solar energy into electrical energy. These systems typically generate

electricity for various applications such as homes, businesses, and industrial facilities. However, connecting PV systems to the grid can lead to certain electrical issues, and harmonics are one of them. Harmonics are unwanted frequency components in the waveform of electrical signals. In grid-connected PV systems, harmonics often occur in the following ways:

• Inverters convert direct current (DC) from PV panels into alternating current (AC) and can introduce harmonics. Inverters typically employ techniques such as pulse-width modulation (PWM), which can generate harmonics.

• When a PV system integrates alternating current into the grid, it can cause harmonic distortions. Harmonics during grid feedback can lead to fluctuations in grid voltage and frequency distortions.

• PV systems often operate alongside other loads present in homes or businesses. If these loads also have nonlinear characteristics, they can contribute to the propagation of harmonics into the grid.

The injection of harmonic components into the grid can lead to undesired effects on the grid and other devices. Therefore, the design and installation of grid-connected PV systems should be done in a way that minimizes harmonic generation. This typically involves the use of filtering and power electronics techniques. Additionally, standards and regulations aim to limit harmonic emissions from PV systems within specific bounds. Total Harmonic Distortion (THD) has separate formulas for current and voltage magnitudes. For current magnitude,

$$THD_I = \frac{\sqrt{\sum_{n=2}^{\infty} I_n^2}}{I_1} = \frac{\sqrt{I_2 + I_3 + I_4 + \cdots + I_n}}{I_1} \tag{1}$$

Where, THD_I represents the total harmonic distortion for current, I_1 represents the effective value of the fundamental frequency current, and In represents the effective value of the nth-order current harmonic. Total harmonic distortion for voltage;

$$THD_V = \frac{\sqrt{\sum_{n=2}^{\infty} V_n^2}}{V_1} = \frac{\sqrt{V_2 + V_3 + V_4 + \cdots + V_n}}{V_1} \tag{2}$$

Where, THDv represents the total harmonic distortion for voltage, V_1 represents the effective value of the voltage at the fundamental frequency, and Vn represents the effective value of the nth-order voltage harmonic. When PV systems are connected to the grid, the presence of nonlinear loads can contribute to the generation of harmonic components. Nonlinear

loads typically include power electronics-based electronic devices, saturated transformers, and gas discharge lamps, all of which belong to the nonlinear load category and often distort the waveform.

PV systems typically convert direct current to alternating current through inverters. These inverters often employ switching techniques, which can introduce irregularities in the waveform. These irregularities can lead to the formation of harmonic components. When nonlinear loads are supplied by a PV system, these loads can also generate harmonic components. Particularly, if nonlinear loads have their own inverters that convert direct current to alternating current, these inverters can contribute to the formation of harmonic components.
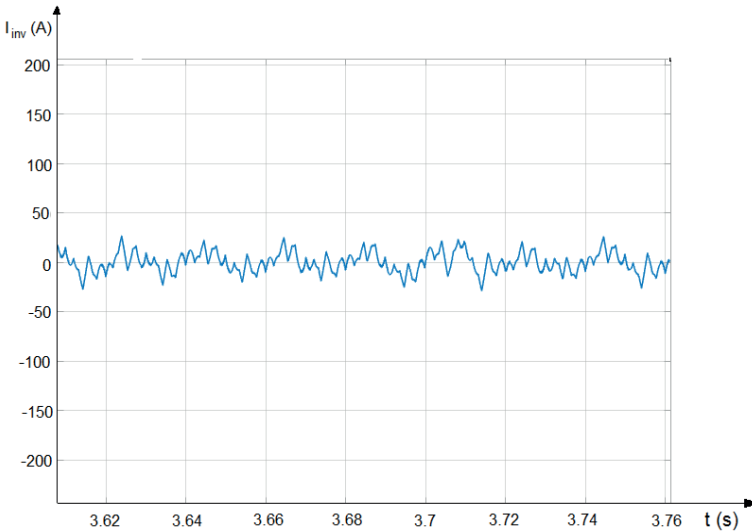
Figure 2 Inverter output current waveform

The presence of harmonic components can lead to undesired effects on grid feedback and other equipment. Therefore, it is crucial to control harmonic components during the design and installation of PV systems. This control is typically achieved through techniques such as filtering and appropriate equipment selection. Managing harmonic components is important not only to enhance the efficiency of PV systems but also to prevent damage to the grid. Hence, considering harmonic components in the design and operation of PV systems is essential.

Table 1. *Effective harmonic components of the inverter output current in the PV system.*

Harmonic Components (In)	Current values of Harmonic Components (I)	Angle Values of Harmonic Components (Degree)
I_1	8.499	-3.851
I_2	4.661	94.59
I_3	1.203	136.3
I_4	3.004	-169.7
I_5	3.363	131.6
I_7	6.134	-71.22
I_{10}	1.109	125.2
I_{11}	2.281	-74.41
I_{13}	0.9266	156.9

If we write the values in Table 1 in analytical form, the following equation is obtained.

$$i(\omega t) = 8.499\mathrm{Sin}(\omega t - 3.851) + 4.661\mathrm{Sin}(2\omega t + 94.59) +$$
$$1.203\mathrm{Sin}(3\omega t + 136.3) +$$
$$\mathrm{Sin}(4\omega t - 169.7) + 3.363\ \mathrm{Sin}(5\omega t + 131.6) +$$
$$6.134\mathrm{Sin}(7\omega t - 71.22 + 1.109\mathrm{Sin}(10\omega t + 125.2) +$$
$$2.281\mathit{Sin}(11\omega t - 74.41) + 0.9266\mathit{Sin}(13 + 156.9) +$$
$$0.4424\mathit{Sin}(17\omega t - 53.17)$$

3.004

The output current and its harmonic components of the inverter in the grid-connected PV system are given in Fig. 3.
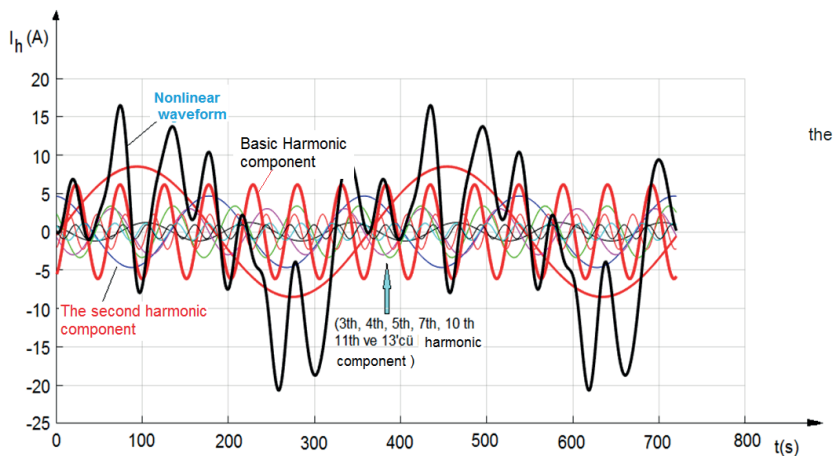
Figure 3. Inverter output current and its harmonic components.

Inverter output current harmonics in solar photovoltaic systems typically vary depending on the system size, design, and the inverter technology used. Inverters generally convert direct current to alternating current, which can

introduce harmonic components. Harmonic components often stem from the nonlinear behavior of electrical devices. Nonlinear loads alter the shape of current and voltage waveforms, thereby generating harmonic components. Inverters fall into this category of loads and can produce harmonic components in their outputs.

The types of inverters commonly used in solar photovoltaic systems can influence the amount of harmonic components present. Different inverter technologies can generate harmonics in varying ways, with some producing fewer harmonic components than others. Therefore, the harmonic profile of a system depends on the characteristics of the inverter used. The presence of harmonic components can affect system performance and potentially harm other devices on the electrical grid or degrade their performance. Hence, it is important to control and limit harmonic components, typically achieved through filtering and power electronics techniques. For the nonlinear waveform shown in Fig. 3, the Total Harmonic Distortion (THD) can be calculated using Eq.(1).

$$THD_I = \frac{\sqrt{\begin{array}{c}4.661^2 + 1.203^2 + 3.004^2 + 3.363^2 + 6.134^2 + \\ 1.109^2 + 1.109^2 + 2.281^2 + 0.9266^2 + 0.4424^2\end{array}}}{8.499}$$
$$= 1.10$$

is found. To reduce this value to the limits accepted by standards, passive filters are necessary. High Total Harmonic Distortion (THD) in photovoltaic systems can typically lead to several negative effects:

• **Efficiency loss in solar PV systems:** High THD levels can reduce the efficiency of photovoltaic inverters. They can have a negative impact on the inverters' ability to accurately convert DC power to AC power.

• **Equipment damage in solar facilities:** High levels of harmonic distortion can lead to damage such as overheating in inverters and other system components. This can shorten equipment lifespan and increase maintenance costs.

• **Damaging the electrical grid:** High THD can potentially harm the electrical grid when feeding back into it. This situation can have adverse effects on other users connected to the grid and may lead to electrical safety issues.

• **System instability:** In some countries, the amount of harmonic distortion injected into the electrical grid by photovoltaic systems must be within specified limits. High THD levels can affect regulatory compliance.

Due to these reasons, controlling harmonic distortion in the design and operation of photovoltaic systems is crucial. This can be achieved through appropriate filtering and power electronics design. The presence of harmonic

components in the output of inverters in grid-connected photovoltaic systems is quite common. Harmonic components are frequency components that cause irregularities deviating the waveform from its sinusoidal shape.

These harmonic components typically stem from the switched nature of inverters. Inverters commonly use Pulse Width Modulation (PWM) technology to convert direct current to alternating current. PWM involves varying the width of pulses to generate the AC signal and utilizes IGBT transistors as switching elements. During the switching process, harmonic components can be generated in the waveform. These harmonics can introduce additional loads to the grid, leading to undesirable effects. For instance, harmonics can hinder the proper operation of other equipment connected to the grid and cause overheating and energy losses.

Therefore, reducing harmonic components during the design and control of inverters is crucial. This is typically achieved through filtering techniques or advanced control strategies. Filtering is a method used to prevent harmonic components from being fed back into the grid. Additionally, selecting the appropriate inverters and placing them correctly can also help reduce harmonic components. Controlling harmonic components should be considered during the design and installation of photovoltaic systems, and necessary measures should be taken to ensure compliance with local regulations and standards.

3. MATLAB/SIMULINK ANALYSIS OF GRID CONNECTED PHOTOVOLTAIC SYSTEMS

MATLAB/Simulink analysis of grid-connected PV systems is commonly used to simulate solar energy systems and evaluate their performance. Such analyses typically include PV panels, inverters, grid connection, and control strategies. Here is a general flow of MATLAB/Simulink analysis that can be used for such an analysis:

- **PV Panel Modeling:** A suitable model is used to simulate the electrical behavior of PV panels. This typically involves mathematical models defined by current-voltage (I-V) and power-voltage (P-V) curves or models based on datasheet specifications.

- **Solar Irradiance Modeling:** A suitable model is used to simulate the spatial and temporal variation of solar irradiance. Solar irradiance is typically predicted based on local climate data and solar movement models.

- **Inverter Modeling:** The inverter is a crucial component that converts DC power input to AC power output. In MATLAB/Simulink, there are models available that represent various types of inverters.

- **Grid Connection:** When the PV system is connected to the grid, this connection should also be modeled. In a grid-connected system, parameters such as grid voltage and frequency are important.

• **Control Strategies:** Various control strategies can be employed to enhance the efficiency of the PV system. These include Maximum Power Point Tracking (MPPT), active power control, reactive power control, and others.

• Performance Analysis: Using MATLAB/Simulink, you can analyze the performance of the PV system in the model. This involves evaluating how the system behaves under various weather conditions.

• **Optimization and Decision Making:** Based on the analysis results, optimization or decision-making processes can be carried out. This is done to enhance system efficiency or determine design parameters.

Matlab/Simulink is a powerful tool for the analysis of photovoltaic systems because it provides flexibility to model the complex interactions of electrical components, control strategies, and various weather conditions. By following this workflow, you can conduct a comprehensive analysis of grid-connected photovoltaic systems in Matlab/Simulink. However, there are some challenges that may be encountered at the connection points of PV systems:

• **Grid Connection:** Connecting PV systems to the electrical grid must comply with local electrical regulations and standards. This may require suitable electrical panels and connection equipment. Additionally, power electronics and energy management strategies should be carefully designed to ensure safe and efficient grid connection.

• **Grounding and Safety**: PV systems must be safely grounded and protected against lightning strikes. Additionally, fire safety measures should be considered. This may involve using appropriate grounding equipment during system installation and integrating fire suppression systems.

• **Environmental Conditions:** PV systems are typically installed in outdoor environments and are exposed to various environmental factors. This includes sunlight, wind, rain, snow, and temperature variations that can affect system performance. Installation and connection point design should be resilient to these environmental conditions.

• **Power Quality Issues:** Connecting PV systems to the grid can lead to power quality issues. Problems such as high total harmonic distortion (THD), voltage fluctuations, and frequency deviations can cause harm to other electrical users and devices in the vicinity. Therefore, appropriate power electronics filtering and regulation strategies should be employed.

To overcome these challenges, the design and installation of PV system connection points must carefully adhere to local regulations, safety standards, and environmental conditions.
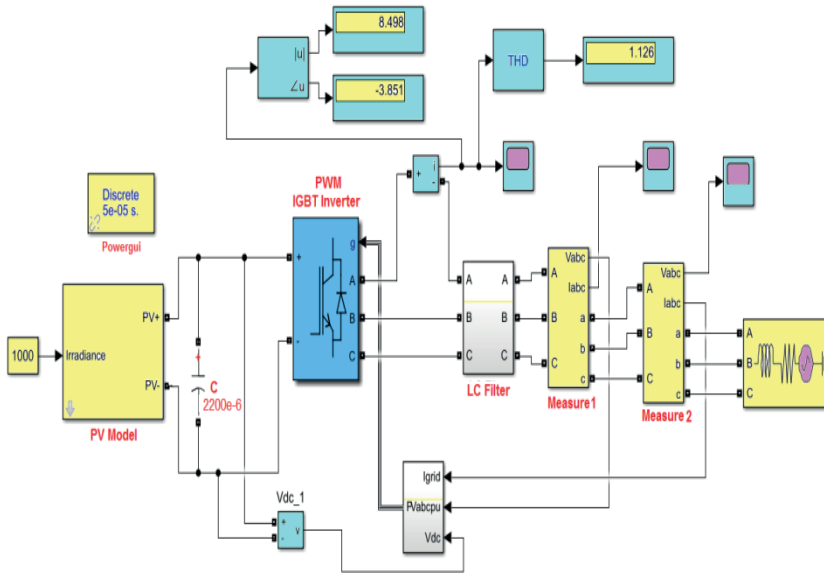
Figure 4: Principle schematic of grid-connected PV system

Grid-connected PV systems in Simulink are typically constructed using a Simulink model. This model includes the electrical generation of the photovoltaic module, MPPT (Maximum Power Point Tracking) control, power converter, and grid connection. The first step is to model the electrical generation of the PV module, which involves capturing the current and voltage generated as the module is exposed to sunlight. This model is created using relevant equations and parameters. There may be some challenges encountered at the connection point of PV systems.

Connecting PV systems to the grid must comply with local electrical regulations and standards. This often requires appropriate electrical panels and connection equipment. Moreover, power electronics and energy management strategies must be carefully designed to ensure safe and efficient grid integration. Overcoming these challenges involves meticulously designing and installing the connection point of PV systems in accordance with local regulations, safety standards, and environmental conditions.

MPPT control ensures that the PV panel finds and operates at its maximum power point. Typically, this is achieved using a PID controller or other control algorithms. The controller monitors the power output of the module and adjusts it to the optimal operating point. The power converter converts the direct current from the photovoltaic panel to alternating current suitable for grid voltage and frequency. Usually, this conversion is accomplished using a DC-DC converter and a DC-AC inverter. The models of these components are integrated into Simulink.
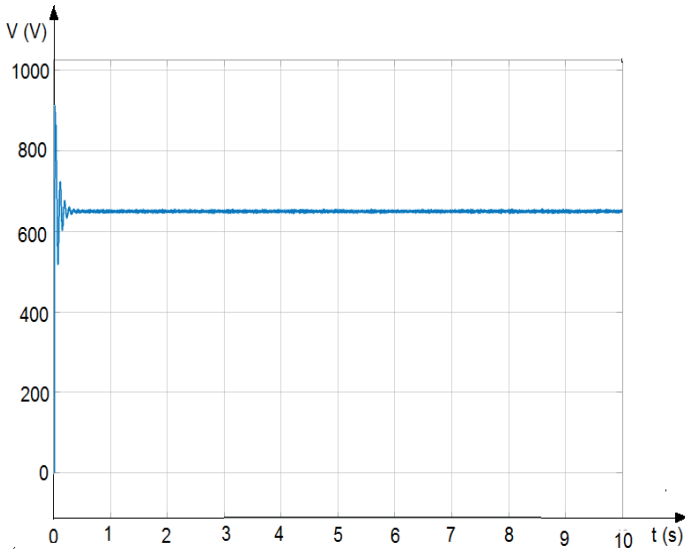
Figure 5 Variation of inverter input voltage

In grid-connected photovoltaic systems, the inverter typically converts the direct current power from photovoltaic (PV) panels, which are DC power sources, into alternating current power. During this conversion, the voltage at the input of the inverter can fluctuate due to factors such as sunlight intensity and angle, which affect the power output from the PV panels.

You can use a capacitor to stabilize the voltage at the input of the inverter. Capacitors are components used to store electrical charge and can mitigate voltage fluctuations. In the context of grid-connected photovoltaic systems, capacitors are typically employed as filters to reduce voltage fluctuations at the input of the inverter. However, the input voltage in grid-connected PV systems is often not constant. Variations in the DC voltage from the PV panels can occur due to changes in sunlight. Consequently, the supply voltage across the capacitor of the inverter will also fluctuate.

As a result, the input voltage to the inverter powered through a capacitor in grid-connected photovoltaic systems can fluctuate, but methods such as MPPT systems and capacitors can be used to mitigate these fluctuations. The output voltage and current magnitudes of the inverter exhibit a nonlinear characteristic, which is why they contain harmonic components.
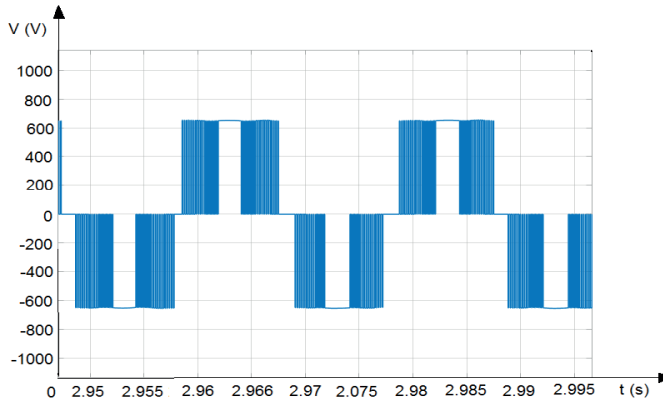
Figure 6 Variation of inverter output interphase voltage in the grid-connected PV system.

In grid-connected photovoltaic systems, inverters typically convert direct current from solar panels into three-phase alternating current to supply energy to the grid. Phase-to-phase voltage variation at the output of inverters is crucial in these systems because such variation can lead to undesirable effects on the grid.

Inverters typically undergo a series of safety and compliance tests before being connected to the grid. These tests include evaluating phase-to-phase voltage variations. Phase-to-phase voltage variation at the output of inverters must comply with limits set by regulatory standards. The management of phase-to-phase voltage variation is usually handled by the control strategies of inverters. Inverters monitor grid voltage and frequency and adjust their outputs accordingly. Moreover, they employ various sensors and control algorithms to minimize phase-to-phase voltage variation.

During the design and installation of photovoltaic systems, appropriately selecting and placing inverters helps in controlling phase-to-phase voltage variations. Additionally, regularly monitoring system performance and conducting maintenance are crucial for maintaining control over phase-to-phase voltage variation.
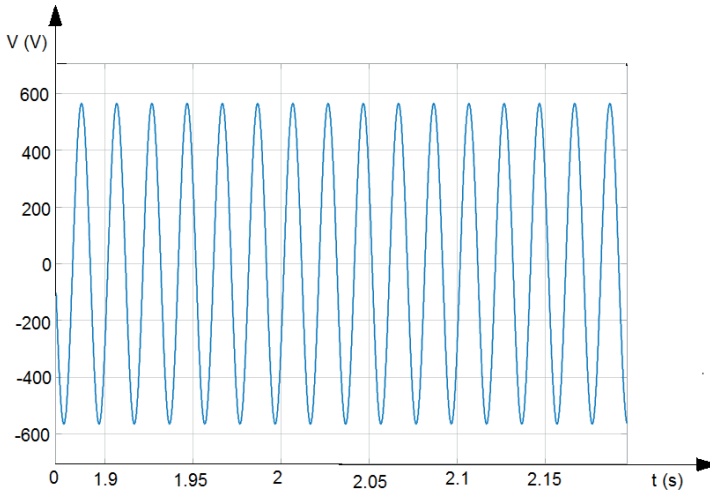
Figure 7 Interphase voltage at the connection point of the PV system

PV systems are typically integrated into three-phase systems when connected to the grid. In this case, phase-to-phase voltage variation is a critical concern that must be carefully controlled. There are several challenges associated with the connection point of photovoltaic systems. Connecting PV systems to the grid must comply with local electrical regulations and standards. This may require appropriate electrical panels and connection equipment. Additionally, power electronics and energy management strategies should be carefully designed to ensure safe and efficient grid connection. Overcoming these challenges requires meticulous attention to the design and installation of the PV system connection point, adhering closely to local regulations, safety standards, and environmental conditions.

PV systems are typically integrated into three-phase systems when connected to the grid. In this case, phase-to-phase voltage variation is a critical concern that must be carefully controlled. There are several challenges associated with the connection point of photovoltaic systems. Connecting PV systems to the grid must comply with local electrical regulations and standards. This may require appropriate electrical panels and connection equipment. Additionally, power electronics and energy management strategies should be carefully designed to ensure safe and efficient grid connection. Overcoming these challenges requires meticulous attention to the design and installation of the PV system connection point, adhering closely to local regulations, safety standards, and environmental conditions.

In a grid-connected PV solar system, the voltage variation between phases is generally important for proper synchronization of the system, control of power factor, and supplying energy to the grid without causing harm. The

voltage variation between phases is controlled and monitored by the inverters in the system. Inverters must operate in synchronization with the grid voltage and frequency, and employ appropriate control strategies to minimize the voltage variation between phases. Inverters typically use Maximum Power Point Tracking (MPPT) technology to manage this change. This technology monitors the output voltage and current of the solar panel to maximize the efficiency of energy conversion from the panel.

In addition, inverters typically monitor and operate according to the grid frequency and voltage. If the voltage deviation between phases is not controlled, it can potentially damage the grid and pose a safety risk. Therefore, it is crucial to consider this factor during the design, installation, and operation of photovoltaic systems.

4. CONCLUSIONS AND SUGGESTIONS

This study conducted an examination on the analysis of grid-connected photovoltaic systems. As solar energy's importance continues to grow, photovoltaic systems emerge as a significant technology in this field. Grid-connected systems operate by connecting to the electrical grid, feeding excess energy into it or drawing energy from it. In the technical analysis of grid-connected photovoltaic systems, performance, efficiency, and harmonic analysis were conducted. It is recognized that grid-connected photovoltaic systems play a crucial role as a sustainable option in energy production, underscoring the importance of analyzing these systems for making informed decisions both technically and economically. Future research is expected to focus on enhancing the performance and reducing the costs of these systems. Grid-connected photovoltaic systems have both positive and negative aspects. The positive aspects are:

- **Clean Energy Production:** PV systems generate electricity from sunlight, providing a clean and environmentally friendly energy source compared to fossil fuels.

- **Low Concrete Requirement**: PV systems are typically installed at ground level or on rooftops, significantly reducing the need for concrete and aiding in the preservation of natural habitats.

- **Local Energy Production:** PV systems consume electricity directly at the point of generation, reducing energy transmission losses and alleviating the load on the grid.

- **Decreasing Costs:** PV panel prices and installation costs have declined over time, making PV systems more accessible and contributing to increased cost-effectiveness.

- **Energy Security:** PV systems provide strong energy security in

regions abundant with sunlight, as they depend on the availability of sunlight.

• **Increased Efficiency:** Replacing PV modules with higher efficiency ones or updating inverters with more efficient models enhances the efficiency of the PV system.

Disadvantages of grid-connected photovoltaic systems:

• **Variable Sunlight:** Solar energy depends on weather conditions and the day/night cycle, which can make it challenging for PV systems to provide a continuous and stable power source.

• **Storage Issues:** Despite advancements in energy storage technologies, limitations remain in storing and accessing solar energy, although these constraints are decreasing.

• **Location and Resource Constraints**: PV systems require suitable space and access to sunlight for installation, which limits their use in certain locations.

• **Integration Challenges:** The integration of PV systems into the grid comes with technical challenges and regulations concerning grid compatibility, safety, and stability.

• **Integration Challenges:** The integration of PV systems into the grid comes with technical challenges and regulations concerning grid compatibility, safety, and stability.

These positive and negative aspects should be considered for the widespread adoption of photovoltaic energy and a more sustainable energy future. With technological advancements and appropriate policy regulations, negative aspects can be mitigated while positive aspects can be enhanced. Additionally, recommendations may include optimizing maintenance routines or making changes in system design to improve reliability and durability.

REFERENCES

1. Yang, B., Li, W., Zhao, Y. & He, X. (2010). Design and Analysis of a Grid-Connected Photovoltaic Power System, in IEEE Transactions on Power Electronics, 25 (4): 992-1000, https://doi.org/10.1109/TPEL.2009.2036432

2. Cai, W., Ren,H., Jiao, Y., Cai, M. & Cheng, X. (2011). Analysis and simulation for grid-connected photovoltaic system based on MATLAB, *2011 International Conference on Electrical and Control Engineering*, Yichang, China, pp. 63-66. https://doi.org/10.1109/ICECENG.2011.6056813

3. Prajapat, K.K., Katariya, A., Kumar, A. & Shukla, S. (2011). Simulation and Testing of Photovoltaic with Grid Connected System, 2011 International Conference on Computational Intelligence and Communication Networks, Gwalior, India, pp. 692-697. https://doi.org/10.1109/CICN.2011.150

4. Mathew, M. & Hossain, J. (2017). Analysis of a grid connected solar photovoltaic system with different PV technologies, 2017 IEEE International Conference on Circuits and Systems (ICCS), Thiruvananthapuram, India, pp. 264-269. https://doi.org/10.1109/ICCS1.2017.8326002

5. Wang, Y.B., Wu,C.S., Liao, H. & Xu, H.H. (2008). Steady-state model and power flow analysis of grid-connected photovoltaic power system, 2008 IEEE International Conference on Industrial Technology, Chengdu, China, pp. 1-6. https://doi.org/10.1109/ICIT.2008.4608553

6. Sreedevi, J., Ashwin, N. & Raju, M.N. (2016). A study on grid connected PV system, 2016 National Power Systems Conference (NPSC), Bhubaneswar, India, pp. 1-6.

7. https://doi.org/10.1109/NPSC.2016.7858870

8. Kumary, S.V.S., Oo, V.A.A.M.T., Shafiullah, G.M. & Stojcevski, A. (2014). Modelling and power quality analysis of a grid-connected solar PV system, 2014 Australasian Universities Power Engineering Conference (AUPEC), Perth, WA, Australia, pp. 1-6.

9. https://doi.org/10.1109/AUPEC.2014.6966605

10. Farhoodnea, M., Mohamed, A., Shareef, H. & Zayandehroodi, (2012). Power quality impact of grid-connected photovoltaic generation system in distribution networks, 2012 IEEE Student Conference on Research and Development (SCOReD), Pulau Pinang, Malaysia, pp. 1-6.   https://doi.org/10.1109/SCOReD.2012.6518600

11. Malla, S.G. (2017). Small signal model of PV power generation system, 2017 IEEE International Conference on Power, Control, Signals and Instrumentation Engineering (ICPCSI),pp.3069-3073, https://doi.org/10.1109/ICPCSI.2017.8392289

12. Ropp, M.E. & Gonzalez, S. (2009). Development of a MATLAB/Simulink Model of a Single-Phase Grid-Connected Photovoltaic System, in IEEE Transactions on Energy Conversion, 24 (1) :195-202.

13. https://doi.org/10.1109/TEC.2008.2003206

14. Tan, R.H.G., P. L. J. Tai, PLJ. & Mok, V.H. (2013). Solar irradiance estimation based on photovoltaic module short circuit current measurement, 2013 IEEE International Conference on Smart Instrumentation, Measurement and Applications (ICSIMA), Kuala Lumpur, Malaysia, pp. 1-4. https://doi.org/10.1109/ICSI-MA.2013.6717943

15. Raghuwanshi, S.S. & Gupta, K. (2015). Modeling of a single-phase grid-connected photovoltaic system using MATLAB/Simulink, 2015 International Conference on Computer, Communication and Control (IC4), Indore, India, pp. 1-5. https://doi.org/10.1109/IC4.2015.7375633

16. Makhlouf, M., Messai, F., Nabti,MK. & Benalla, H..(2012). Modeling and simulation of grid-connected photovoltaic distributed generation system, 2012 First International Conference on Renewable Energies and Vehicular Technology, Nabeul, Tunisia, pp. 187-193.

17. https://doi.org/10.1109/REVET.2012.6195269

18. Rustemli, S. & Dincer, F. (2011). Modeling of Photovoltaic Panel and Examining Effects of Temperature in Matlab/Simulink, Electronics and Electrical Engineering, 3(109), 35-40. https://doi.org/10.5755/j01.eee.109.3.166

19. Kocatepe, C., Uzunoğlu, M., Yumurtaci, R., & Arıkan, O. (2003). Elektrik Tesislerinde Harmonikler, Birsen Yayınevi, İstanbul.

20. recent works (2024). Single stage grid connected pv system (https://www.mathworks.com/matlabcentral/fileexchange/112455-single-stage-grid-connected-pv-system), MATLAB Central File Exchange. Retrieved April 2, 2024.https://doi.org/10.1109/ICA-ACCA.2018.8609715

21. Babu, C., Kumar, D.G., Sireesha, N.V. et al., (2023).   Modeling and Performance Analysis of a Grid-Connected Photovoltaic System with Advanced Controller Considering Varying Environmental Conditions, International Journal of Energy Research, https://doi.org/10.1155/2023/1631605

22. Ropp, M.E & Gonzalez, S.(2009). Development of a Matlab/Simulink Model of a Single-Phase Grid-Connected Photovoltaic System, in IEEE Transactions on Energy Conversion, 24 (1): 195-202. https://doi.org/10.1109/TEC.2008.2003206

23. Yang, B., Li,W., Zhao,Y, and He, X.(2010) Design and Analysis of a Grid-Connected Photovoltaic Power System, in IEEE Transactions on Power Electronics, 25(4), 992-1000, https://doi.org/10.1109/TPEL.2009.2036432

24. Pietruszko, S.M., Fetlinski, B, and Bialecki, M.(2009) "Analysis of the performance of grid connected photovoltaic system, 2009 34th IEEE Photovoltaic Specialists Conference (PVSC), Philadelphia, PA, USA, 48-51, doi: https://doi.org/10.1109/PVSC.2009.5411757.